2020년 8월
석사학위 논문

MWCNT/Fe_3O_4 이성분 나노유체의 대류열전달 특성에 대한 실험적 연구

조선대학교 대학원

기 계 공 학 과

졸자르갈 나란키쉬그

MWCNT/Fe_3O_4 이성분 나노유체의 대류열전달 특성에 대한 실험적 연구

Experimental study on the convective heat transfer characteristics of MWCNT/Fe_3O_4 hybrid nanofluid

2020년 8월 28일

조선대학교 대학원

기 계 공 학 과

졸자르갈 나란키쉬그

MWCNT/Fe_3O_4 이성분 나노유체의 대류열전달 특성에 대한 실험적 연구

지도교수 : 조 홍 현

이 논문을 공학석사 학위신청 논문으로 제출함

2020년 5월

조선대학교 대학원

기 계 공 학 과

졸자르갈 나란키쉬그

졸자르갈 나란키쉬그의 석사학위 논문을 인준함

위원장 조선대학교 교수 오 동 욱 ㊞
위 원 조선대학교 교수 박 정 수 ㊞
위 원 조선대학교 교수 조 홍 현 ㊞

2020년 6월

조선대학교 대학원

Contents

List of Figures

List of Tables

Nomenclature

C_p	: Specific heat capacity kJ/kgK
A	: Area, m^2
w	: Weight g
P	: Power, W
V	: Voltage, Volts
I	: Current, Amp
Q	: Heat flow, Watts
T	: Temperature, °C
D	: Inner diameter of test section, m
L	: Length of test section, m
h	: Convective heat transfer coefficient, W/m^2K
m	: Mass flow rate, kg/s
k	: Thermal conductivity, W/mK
q	: Heat flux, W/m^2
EG	: Ethylene Glycol
$MWCNT$	: Multi-walled carbon nanotube
Re	: Reynolds number

Greeks

ϕ	: Weight concentration, wt%
ρ	: Density, kg/m^3
μ	: Viscosity, kg/ms
$\triangle P$	: Pressure drop, kPa

Subscript

bf	: Base fluid
i	: Inlet
o	: Outlet
w	: Wall temperature
b	: Bulk temperature
max	: Maximum
min	: Minimum
nf	: Nanofluid
np	: Nanoparticle

Abstract

Experimental Study on Convective Heat Transfer Characteristics of MWCNT/Fe_3O_4 Hybrid Nanofluid

Zoljargal Narankhishig
Advisor: Prof. Honghyun Cho, PhD.
Graduate School of Chosun University

The forced convective heat transfer is the key of heat transfer processes affected by the flow of working fluid. In this study, the convective heat transfer coefficient and friction factor of MWCNT, Fe_3O_4, and MWCNT/Fe_3O_4 hybrid nanofluids was investigated experimentally in a heating circular pipe at different Reynolds numbers (1000, 1200, 1400 and 1600). The weight concentrations of 0.025wt%, 0.05wt%, 0.1wt% and 0.2wt% was used in the MWCNT, Fe_3O_4, and MWCNT/Fe_3O_4 hybrid nanofluids, and mass mixing ratio of the MWCNT/Fe_3O_4 hybrid nanofluid was fixed by 1:1 between MWCNT and Fe_3O_4 nanoparticles.

This study is to introduce the basic concept of convective heat transfer, nano-sized nanoparticles, and main problematic prediction of convective heat transfer. First, previous studies reviewed and summarized in the first part. In the second, synthesis method of Fe_3O_4 nanoparticle, the preparation method of hybrid nanofluid, measurement techniques of thermal conductivities of nanofluids, convective heat transfer experimental setup, and method are presented. In the third, considering all these mentioned elements, enhancement of convective heat

transfer coefficient, Nusselt numbers, pressure drop, and friction factors in MWCNT, Fe_3O_4, and MWCNT/Fe_3O_4 hybrid nanofluids were comprehensively analyzed. Generally, the convective heat transfer coefficient increases with the Reynolds number and weight concentration of nanofluids, so these phenomenon was verified in this study.

The convective heat transfer coefficient of MWCNT/Fe_3O_4 hybrid nanofluid was ranged from 1914.3 to 1988.4 W/m^2K, which was 6%-12.4% higher than that of the base fluid. The maximum improvement in the convective heat transfer coefficient was presented at 0.1wt% MWCNT/Fe_3O_4 hybrid nanofluid and Reynolds number of 1600, which was 12.4% higher than that of base fluid. The convective heat transfer coefficient of MWCNT/Fe_3O_4 hybrid nanofluid was 1914.3 W/m^2K, 1958.5 W/m^2K, and 1988.4 W/m^2K, respectively, at weight concentrations of 0.025wt%, 0.05wt%, and 0.2wt%, which were 6%, 8.5%, and 10.1% increased one compared to those of the base fluid. The Fe_3O_4 nanocomposite synthesized by using the co-precipitation method, which has a magnetic property and has a high potential to improve its thermal properties by adding high thermal conductivity material of MWCNT nanoparticles to Fe_3O_4 nanofluid. The adding of Fe_3O_4 nanoparticles into the base fluid can reduce the thermal conductivity of Fe_3O_4 nanofluid. It may increase the viscosity of the high concentration of nanofluids, which increases the viscous of the layer, therefore the friction factor increases. The MWCNT/Fe_3O_4 hybrid nanofluid are more effective in the increase the convective heat transfer coefficient compared to single MWCNT and Fe_3O_4 nanofluids.

I. Introduction

1.1 Background

A conventional heat transfer is the most important study of heat transfer process used in an engineering fields, numerous industries such as cooling/heating applications and other industrial systems. The convective heat transfer can improve the characteristics of heat transfer through the widespread applicability or variation of the heat exchanger elements or other heat transfer applications. Most studies have been conducted to improve the convective heat transfer performance and to consider the possibility of improving the convective heat transfer characteristics through advanced nanotechnology as described in the atomic and molecular scales of nanoparticles using micro-scale materials, as well as molecular technologies using a nano-sized nanopaticles. Nanofluids improve the heat transfer of conventional working fluids such as water, ethylene glycol and oil by adding nano-sized nanoparticles with high thermal conductivity to improve their nanofluid thermal properties. Specifically, nano-sized particles have at least two dimensions between 1 and 100 nanometres. On this scale, interatomic forces become large, and must be considered when conducting studies to characterize the experiment and model the behaviors of nanomaterials. Fig. 1.1 shows the combination of nanoparticles and biomolecule on a nanoscale [1].

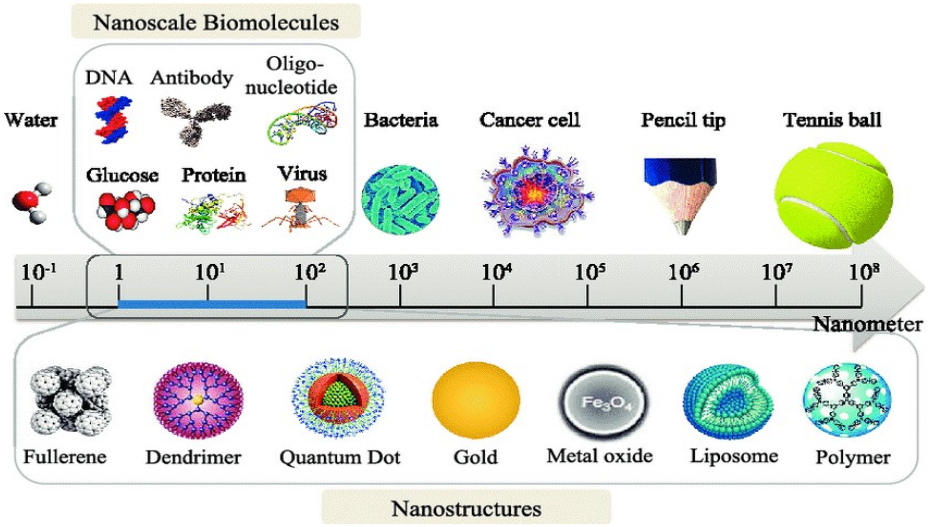

Fig. 1.1 Nanoscale combination of nanoparticle and biomolecule [1]

Therefore, A mixture of nano-sized nanoparticles and a conventional working fluid is called a nanofluid. The nanofluids have a higher thermal properties and a higher thermal conductivity than a base fluids of water, ethylene glycol and oil. Firstly, Choi and Eastman [2] investigated the basic concept of nanofluids in 1995. Subsequently, a large number of researchers developed the effects of thermal properties of nanofluids on the improvement of convective heat transfer of various nanofluids with nanoparticles, such as Al_2O_3, TiO, CNT, SiO_2, CuO, and Fe_3O_4, respectively.

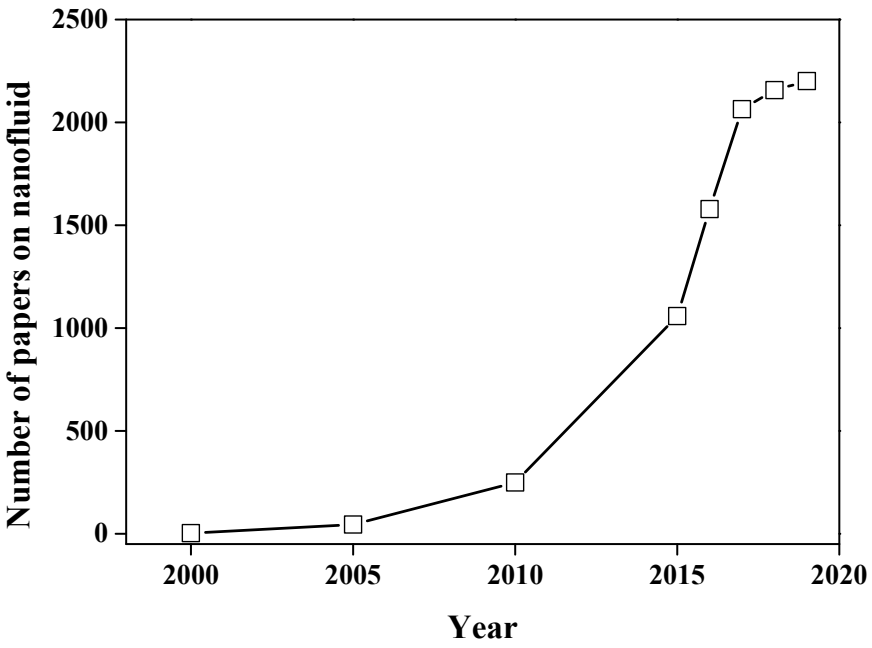

Fig. 1.2 Number of papers related to nanofluids

Fig. 1.2 shows the numerous nanofluid related papers published over the last decade. Research into nanofluids has grown sharply over the last 20 years. Nowadays, many researchers are focusing on a new type of nanofluid by mixing magnetic particles (cobalt, nickel, and iron) and a conventional working fluid (such as water and glycol), called Ferrofluids (Fe_3O_4). In general, ferrofluids can be used in engineering applications such as heat exchangers, microdevices, refrigeration, turbomachinery, chemical reactors and air conditioning systems. Nanofluids with magnetic nanoparticles have been shown to improve thermophysical properties compared to non-magnetic nanofluid and conventional working fluids.

1.2 Previous studies

The nanofluid is the fluid contained nano-meter sized nanoparticles in the conventional working fluid such as water, ethylene glycol, oils. Nanoparticles with their superior thermal properties, when suspended in the conventional working fluids, find engineering applications for the convective heat transfer of fluids in mechanical engineering. Cieslinski [3] investigated the convective heat transfer potential of an Al_2O_3/water-EG nanofluid at the concentrations ranging from 0.1vol% to 1vol% in the transient and turbulent flow region. The convective heat transfer coefficient was shown the increase in the nanoparticle concentration which reduces the convective heat transfer coefficient, and a maximum decrement of convective heat transfer coefficent was approximately 25% for a base fluid of 50:50 water:EG mixing ratio at concentration of 1vol%. Minakov et al. [4] have studied the convective heat transfer of a CuO/water nanofluid at various concentrations in the laminar flow region. Their results conclude that the convective heat transfer coefficient of CuO/water at concentration of 2vol% with a constant Reynolds number improved by 40% compared to that of the base fluid of water. For this, increment of viscosity was shown with the nanoparticle concentration, which is due to the high pumping power. In addition, Gupta et al. [5] investigated the convective heat transfer of MWCNT/DI-water at concentration ranging from 0.05wt%–0.5wt% with a laminar flow region. The maximum improvement in convective heat transfer coefficient was 77.6% in the concentration of 0.5wt% MWCNT/Di-water nanofluid with the flow velocity of 0.232 m/s as compared to the base fluid of water. Numerous studies on the

convective heat transfer in various nanofluids have been conducted using a wide range of nanoparticles such as TiO_2, CuO, Al_2O_3, SiC, SiO_2, and MWCNT nanoparticles. [6-14]. Shin et al. [15] studied the convective heat transfer of Al_2O_3, CuO, and TiO_2 nanoparticles under three dimensional simulation in rectangular microchannels. They analysed that the local convective heat transfer coefficient increases as the nanoparticle concentration increases according to the type of nanoparticles applied. Oztop et al. [16] numerically studied the effects of the temperature distribution of Al_2O_3 and TiO_2 nanofluids in an inclined square enclosure. An improvement in the convective heat transfer coefficient is shown at a high concentration, and the heat transfer rate increases separately with the types of nanoparticles. The effect of the improved convective heat transfer coefficient is particularly clarity for low Rayleigh numbers. Kalteh et al. [17] analyzed the convective heat transfer coefficient Al_2O_3, TiO_2, Ag, and CuO nanofluids in a square cavity with the triangular heat source. Increasing the concentration leads to an increase in the average Nusselt number for all nanofluids, and the convective heat transfer coefficient of an Al_2O_3 nanofluid is greater than that of a TiO_2 nanofluid. The maximum Nusselt number shows on the top wall at the concentration of 5vol% with Al_2O_3. Azizian et al. [18] numerically and experimentally studied the effects of an external magnetic field of Fe_3O_4/Di-water in convective heat transfer coefficient under a laminar flow region. They concluded that the maximum convective heat transfer coefficient of magnetite nanofluids could be increased about 300% compared to that without the magnetic field.

Nowadays, most convective heat transfer investigations have been conducted with high concentrations of oxide nanoparticles, which can increase the viscosity

of nanofluid and pumping power of the working fluid. Sufficient energy can be transferred to low concentrations of nanofluids because the thermal conductivity of carbon nanoparticles is higher than the thermal conductivity of oxide nanoparticles [19,20]. Therefore, researchers found that the convective heat transfer enhancement of magnetic nanofluids has shown significant changes in magnetic field [21-26]. Goharkhah et al. [27] examined the convective heat transfer of Fe_3O_4 nanofluid based water in a uniformly heated parallel plate channel with different magnetic field intensities. They concluded that the non-magnetic field, the convective heat transfer coefficient improved by 24.9% and 37.3% at constant and alternating magnetic fields. Yarahmadi et al. [28] studied the convective heat transfer of Fe_3O_4/Di-water in a circular cross-section tube at constant heat flux with a laminar flow region. Maximum improvement of convective heat transfer coefficient was shown in the last segment of the experiment with applied magnetic field on a Fe_3O_4/Di-water nanofluid. At the concentration of 5vol% ferrofluid with a frequency of 50 Hz at Reynold number of 465, a highest improvement in convective heat transfer was 19.8% in the last segment of experiment with the magnetic field as compared to the non-magnetic field. Hatami et al. [29] investigated the convective heat transfer of Fe_3O_4/water nanofluid in a horizontal tube and compared to and without a magnetic field. No effect on convective heat transfer improvement were shown by applying the low magnetic field strenght at a nanoparticle concentration of 0.1vol%. Important improvements in convective heat transfer improvement have been observed in order to increase one of these factors. The convective heat transfer coefficient also decreased with increase in the Hartmann number at the invariant concentration and an increase in the nanoparticle concentration of the nanofluid

which was shown at the constant Hartmann number. This is caused by the action of an applied the presence of a magnetic field, which decentralizes the Brownian motion of nanoparticles. Currently, several researchers are experimentally investigating improved nanofluid dispersion stability. However, when a magnetic nanofluid dispersed by mixing two nanoparticles in a conventional working fluid is used as a hybrid working fluid in a thermal system, the consideration should be given to the consistency of each nanoparticle for its thermal performance with the conventional working fluid. The convective heat transfer characteristics of hybrid nanofluid have been experimentally studied and several results of a preparatory study on the convective heat transfer of hybrid nanofluids were introduced. A new type of nanofluid that is formed by dispersing two or more single nanoparticles in the conventional working fluid can be provided with a hybrid nanofluid. Hybrid nanofluids also have a high thermal properties than a single nanofluid, which disperses one type of nanoparticle.

Numerous studies in the field of hybrid nanofluids have not yet been presented with an acceptable model for various hybrid nanofluids [30-37]. Alsarraf et al. [38] have recently studied simultaneously the convective heat transfer of MWCNT-Fe_3O_4/water hybrid nanofluid with a laminar flow region. The average increase in Nusselt number and pressure drop of a hybrid nanofluid which is containing 0.9vol% and 1.35vol% with magnetite and CNT under a magnetic field were 109.3% and 25.02%, compared without a magnetic field. They conclude that the Nusselt number and pressure drop of the MWCNT-Fe_3O_4/water nanofluid were improved under magnetic conditions. The previously described findings and the improvements in the convective heat transfer of various nanofluids described in other studies are summarized in Table 1.1.

Table 1.1 Summary of studies on convective heat transfer of various nanofluid

Authors	Nanoparticles	Findings
Chiney et al. [6]	Al_2O_3	The improvement is around the 10-60% higher than the base fluids, higher nanoparticle concentration with higher flow rates.
Anoop et al. [7]	Al_2O_3	The improvement of convective heat transfer coefficient was 31% at axial distance of x/D = 63, whereas it increased by 25% and 10% at x/D = 147 and 244, respectively.
Yu et al. [8]	SiC	The improvement convective heat transfer coefficient was around 14-32% higher than standard single-phase turbulent convective heat transfer correlation.
Mehrjou et al. [9]	CuO	The convective heat transfer coefficient of nanofluids at triangular duct is increased as the nanoparticle concentrations increases.
Heris et al. [10]	Al_2O_3, CuO	The convective heat transfer improves with increasing concentrations and Peclet number. Al_2O_3/water nanofluid shows more improvement of convective heat transfer compared with CuO/water nanofluid.
Mangrulkar et al. [11]	Al_2O_3, CuO	The maximum improvement of Al_2O_3/water nanofluid was around 52%, and CuO/water was around 60%.
Kumaresan et al. [12]	MWCNT	The Prandtl number decreases with increase the temperature for all concentration of the nanofluids with MWCNT due to decrease in the viscosity of the MWCNT nanofluids.
Wen and Ding [13]	TiO_2	The convective heat transfer coefficient decreases with increase some deterioration as well as nanoparticle concentrations.
Ferrouillat et al. [14]	SiO_2	The improvement of convective heat transfer increases with the concentration as well as Nusselt number from 10% to about 50% when

		volume concentration ranged from 2.3% to 18.9%.
Ghofrani et al. [21]	Fe_3O_4	The improvement of convective heat transfer increases by 27.6%±1.22% at a Reynolds number of 80 with an alternative magnetic field
Sha et al. [22]	Fe_3O_4	The maximum improvements of convective heat transfer were 4.2% and 8.1% with applying the constant magnetic field.
Asfer et al. [23]	Fe_3O_4	The improvement of thermal conductivity of Fe_3O_4 resulting from the formation of chainlike clusters of IONPs at magnetic field.
Sadrhosseinia et al. [24]	Fe_3O_4	To increasing concentration has a better effect on convective heat transfer improvement ranged from 50 to 75% which are due to the increase of heat conduction at higher volumetric ratios.
Guzei et al. [25]	Fe_3O_4	The convective heat transfer coefficient of a Fe_3O_4 nanofluid with a nanoparticle concentration of 0.25vol% increases by 35% relative to the base fluid with the magnetic field action applied by three magnets.
Ashjaee et al. [26]	Fe_3O_4	The maximum improvement of convective heat transfer was 14% compared to the pure water at applied magnetic field.
Shahsavar et al. [30]	CNT-Fe_3O_4	The maximum improvement of 62.7% was improved for hybrid nanofluid containing 0.9vol% Fe_3O_4 and 1.35vol% CNT at Reynolds number of 2190.
Shi et al. [31]	CNT-Fe_3O_4	The improvement of convective heat transfer increase at high magnetic field strength. it improved from 6.7% to 18.4% at the external magnetic field strength increased from 5 to 40 mT.
Takabi and Shokouhmand	Al_2O_3-Cu	The average increase of Nusselt number in Al_2O_3-Cu/water hybrid nanofluid is 32.07% and

[32]		the amount for the average increase of friction factor is 13.76% compared to pure water.
Balla et al. [33]	CuO, CuO-Cu	Hybrid nanofluids show great improvement in Nusselt number for 2CuO-1Cu and 1CuO-2Cu are 35% and 30% in compare with water
Labib et al. [34]	CNT-Al_2O_3	The improvement of convective heat transfer coefficient of 0.05vol% CNTs+0.6vol% Al_2O_3-water and 0.05vol% CNTs+1.6vol% Al_2O_3-water are 22.8% and 59.86% compared to 0.05vol% CNTs-water nanofluids
Minea et al. [35]	CuO-Cu	The convective heat transfer coefficient of 1%vol 1CuO-2Cu nanofluid was improved by 3.28 times than pure water. The Nusselt number for 1CuO-2Cu nanofluid showed improvement of 129% compared to pure water
Uysal et al. [36]	Diamond-Fe_3O_4	The improvement in convective heat transfer coefficient of 0.2vol% diamond-Fe_3O_4 hybrid/water nanofluid was 29.96% at Reynolds number of 1000
Al-Balushi et al. [37]	Fe_3O_4, $CoFe_2O_4$, Mn-$ZnFe_2O_4$, SiO_2	Those nanofluids have higher convective heat transfer coefficient than water based base fluids. The kerosene based nanofluids showed higher convective heat transfer improvement as an engine oil based nanofluids which show lower heat transfer improvement. Mn-$ZnFe_2O_4$-Ke nanofluid has a higher convective heat transfer coefficient than other types of nanofluids

1.3 Objectives of this study

The representative thermal properties and manufacturing method of nanofluids are briefly introduced, and the convective heat transfer characteristics of the MWCNT/Fe_3O_4 hybrid nanofluid is investigated and their findings discussed. The previous investigations suggested that the Fe_3O_4 nanofluid has a high potential to improve its thermal properties by adding additional MWCNT nanoparticles into nanofluid due to the significant thermal and rheological characteristics of MWCNT nanoparticles. Most of the studies that investigated the convective heat transfer of nanofluids compared the convective heat transfer coefficient of nanofluid with the base fluid; however, several studies can be found with other methods. In previous studies, limited research studies have been reported on the convective heat transfer using MWCNT/Fe_3O_4 hybrid nanofluids which have been shown to be very good thermophysical properties. For that reason, the convective heat transfer characteristics of the MWCNT/Fe_3O_4 nanofluid are investigated and their enhancement results discussed.

The objective of this study is to investigate the convective heat transfer coefficient and the pressure drop of MWCNT, Fe_3O_4, and MWCNT/Fe_3O_4 hybrid nanofluids, which is based on the fluid of EG/Water=20:80 at various weight concentrations ranging from 0.025wt% to 0.2wt%. The experiments were conducted according to the nanofluid of MWCNT, Fe_3O_4, and MWCNT/Fe_3O_4 hybrid nanofluid at Reynolds numbers were ranged from 1000 to 1600 in the laminar flow region. Furthermore, the convective heat transfer coefficient and pressure drop as a function of Reynolds number, nanoparticle concentrations were investigated.

Achieving the enhancement of convective heat transfer and findings are considered to be the experimental analysis.

Ⅱ. Experimental setup and method

2.1 Synthesis of Fe_3O_4 nanoparticles

The co-precipitation method was used in this experiment to synthesize the Fe_3O_4 nanoparticles. For co-precipitation method, the mixture of ferrous chloride ($FeCl_2$) and ($FeCl_3$) iron chloride were stirred in magnetic field at the temperature of 50°C. During the stirring procedure, the aqua ammonia solution (NH_4OH) was added drop-wise to raise at the temperature of 50°C. At this temperature, the solution color was changed from brown to black when adding the aqua ammonia solution (NH_4OH).

Afterwards, the black nanoparticles were magnetically separated from the ammonium solution using the permanent magnet and washed with distilled water more than three times. Separated Fe_3O_4 nanoparticles were coated with an aqueous poly solution (acrylic acid) pumped by a vacuum pump at the temperature of 90°C for 1 hr. After the coating process, the mixture of Fe_3O_4 and poly solution (acrylic acid) was cooled until its temperature reached the ambient temperature and dried in a vacuum filter. Fig. 2.1 shows the process of synthesizing and coating of Fe_3O_4 nanoparticles.

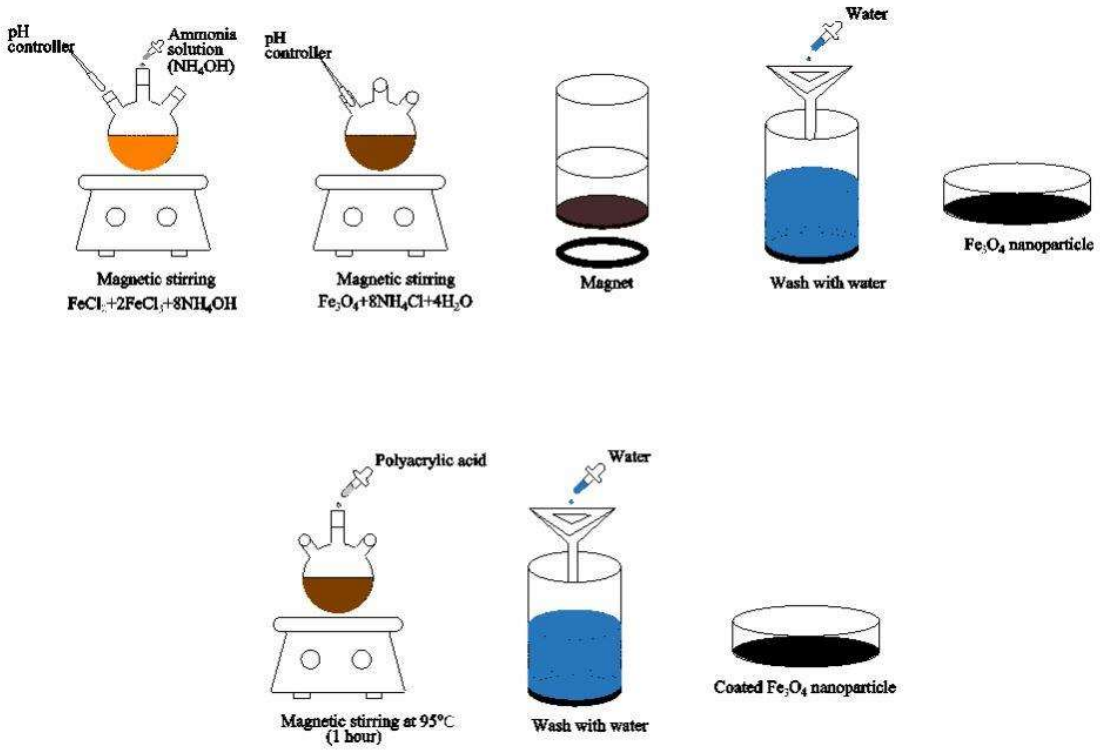

Fig. 2.1 The developed co-precipitation method of Fe_3O_4 nanoparticle

2.2 Preparation method of MWCNT/Fe_3O_4 hybrid nanofluid

In this experiment, a two-step method was used for the manufacture of continuously circulating nanofluids and ultrasonic dispersion. Continuous circulation of ultrasonic dispersion is a process which a mixture is continuously dispersed in a fluid while ultrasonic dispersion and stirring is performed. The two-step manufacturing method is shown in Fig 2.2. Two different nanoparticles (US nano, Inc) used in this study. To disperse nanoparticles, mixing ratio of the base fluid of EG/Water was 20:80 solution. A high concentrated nanofluid was added to the base fluid EG/Water=20:80 and stirred in a pre-mixer for 1 hr, then mixed again in the continuous ultrasonic processor for 2 hr after the pre-mixed nanofluid. To disperse Fe_3O_4 nanoparticles in nanofluid uniformly, the chemical agent poly solution (acrylic acid) was used to coat the surface of Fe_3O_4 nanoparticle. Similar procedures were followed for the preparation of all concentrations of MWCNT or Fe_3O_4 nanofluids based on the base fluid of EG/Water=20:80, in this study. The nanoparticle mixing ratio of MWCNT/Fe_3O_4 hybrid nanofluid was fixed at weight mixing ratio of 1:1, and also weight concentrations of Fe_3O_4, MWCNT, and MWCNT/Fe_3O_4 hybrid nanofluids were 0.005wt%, 0.05wt%, 0.1wt% and 0.2wt%, respectively. Thermo-physical properties of MWCNT, Fe_3O_4 nanoparticles, nanofluids and base fluid EG/Water=20:80 of properties are presented in Tables 2.1 and 2.2.

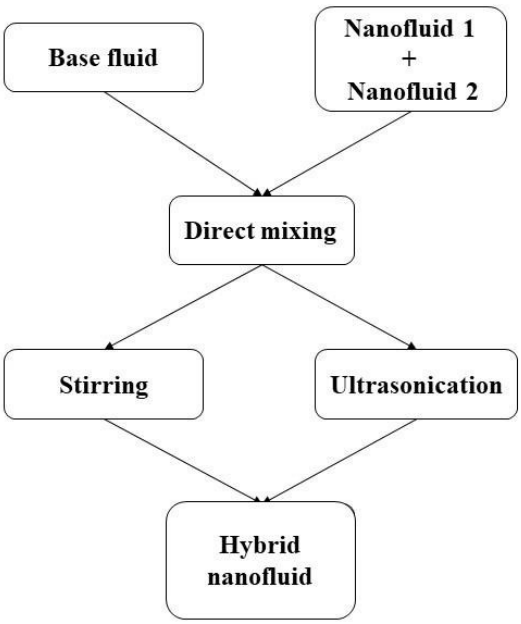

Fig. 2.2 Preparation of hybrid nanofluid using a two-step method

Table 2.1 Thermo-physical properties of MWCNT and Fe_3O_4 nanoparticles

	MWCNT	Fe_3O_4
Purity (%)	>95	99.5+%
Outside diameter (nm)	10-20	15-20
Inside diameter (nm)	5-10	-
Length (μm)	10-30	-
Color	Black	Dark Brown
Electrical conductivity (s/cm)	100	-
Tap density (g/cm^3)	0.22	4.8-5.1
True density (g/cm^3)	~2.1	-

Table 2.2 Thermo-physical properties of working fluids at different weight concentrations

Working fluid	wt%	vol%	Density (kg/m^3)	Specific heat (kJ/kgK)	Viscosity (kg/ms)
EG/Water (20:80)	21.7	20	1027.9	3.826	1.46
MWCNT	0.025	0.019	1034	3747.1	0.00105
	0.05	0.038	1040.2	3668.2	0.00110
	0.1	0.076	1052.4	3510.4	0.00124
	0.2	0.152	1076.9	3194.8	0.00158
Fe_3O_4	0.025	0.005	1048.4	3746.6	0.00101
	0.05	0.010	1068.9	3667.2	0.00102
	0.1	0.020	1110	3508.4	0.00105
	0.2	0.040	1192	3190.8	0.00110
MWCNT/Fe_3O_4 hybrid nanofluid	0.025	0.024	2134.97	1169	0.00107
	0.05	0.048	2135.05	1144	0.00117
	0.1	0.096	2135.2	1094	0.00144
	0.2	0.192	2135.5	996	0.00223

The MWCNT/Fe_3O_4 hybrid nanoparticles were prepared by mixing ratio of 1:1 and weight concentrations ranged from 0.025wt% to 0.2wt%, respectively. The weight concentrations of nanoparticle were estimated by Eq. (1).

$$w_{nf} = \left(\frac{\phi}{100-\phi}\right)\left(\frac{\rho_{nf}}{\rho_{bf}}\right)w_{bf} \tag{1}$$

where ϕ is the weight concentration of nanofluid, ρ_{bf} and ρ_{np} are the mass of base fluid of EG:Water=20:80 and nanoparticles.

Fig. 2.3 presents the transmission electron microscopy (TEM) image of MWCNT, Fe_3O_4 and MWCNT/Fe_3O_4 hybrid nanoparticles, the diameter of the nanoparticles ranged between 10 and 20 nm, which clearly indicates the matching size and structure of the nanoparticles. In Fig. 2.4, X-ray diffraction (XRD) pattern of the MWCNT, Fe_3O_4 and MWCNT/Fe_3O_4 hybrid nanocomposites. The XRD pattern analysis of nanocomposites used in this study reveals sharp density peaks at 25.5° , which is a typical pattern of MWCNT, Fe_3O_4 and MWCNT/Fe_3O_4 hybrid nanocomposite. As shown in Fig. 2.5, no nanoparticle deposition has occurred in the MWCNT, Fe_3O_4 and MWCNT/Fe_3O_4 hybrid nanofluids which indicate higher dispersion stability. Increasing the concentrations of nanofluid can be shown the change of color of nanofluid.

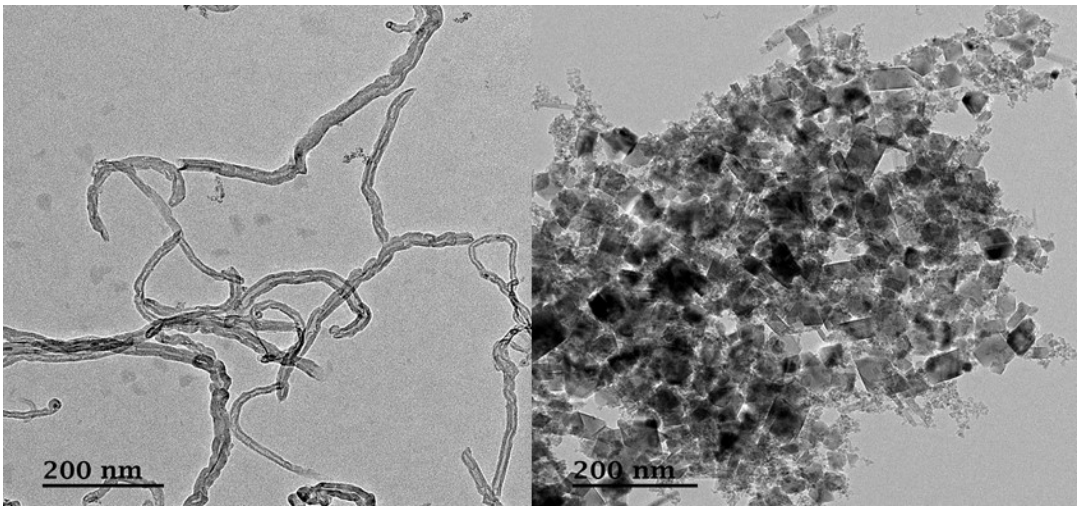

(a) MWCNT nanoparticle (b) Fe_3O_4 nanoparticle

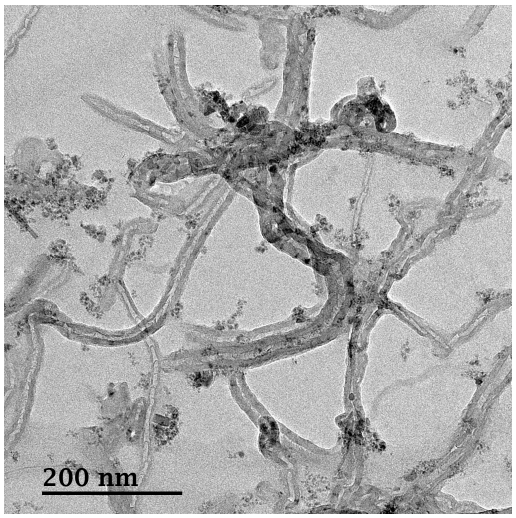

(c) MWCNT/Fe_3O_4 nanoparticle

Fig. 2.3 TEM images of (a) MWCNT nanoparticle, (b) Fe_3O_4 nanoparticle, and (c) MWCNT/Fe_3O_4 hybrid nanoparticle

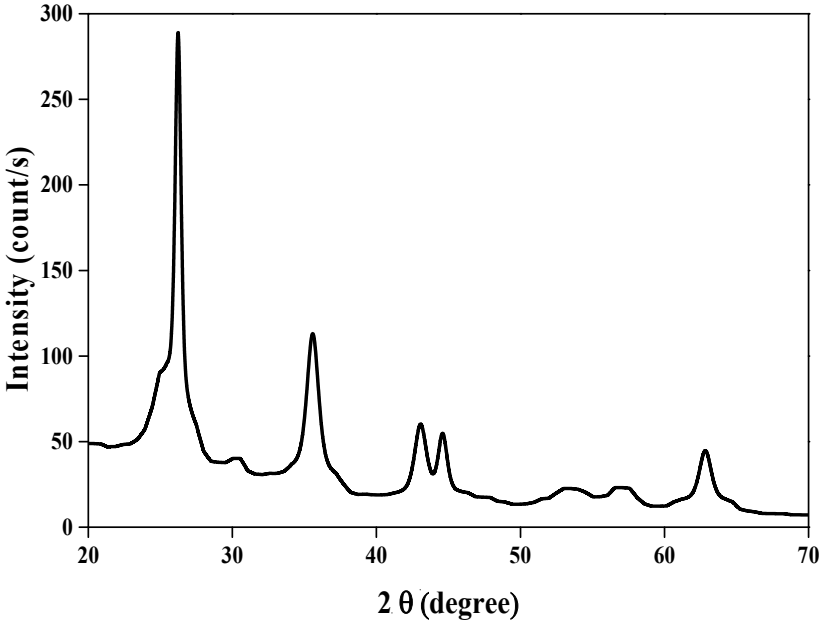

(a) MWCNT nanoparticle

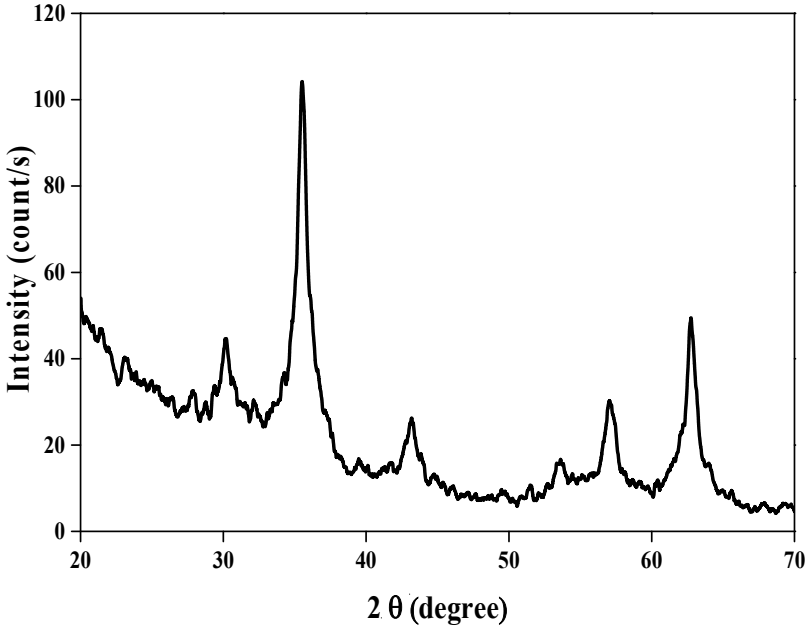

(b) Fe_3O_4 nanoparticle

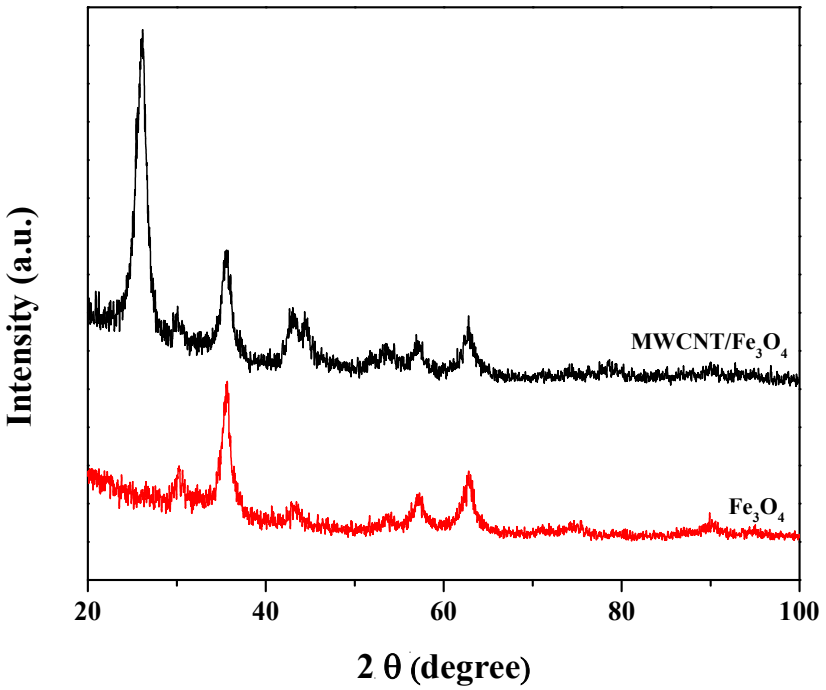

(c) MWCNT/Fe_3O_4 hybrid nanoparticle

Fig. 2.4 XRD images of (a) MWCNT nanoparticle, (b) Fe_3O_4 nanoparticle and (c) MWCNT/Fe_3O_4 hybrid nanoparticle

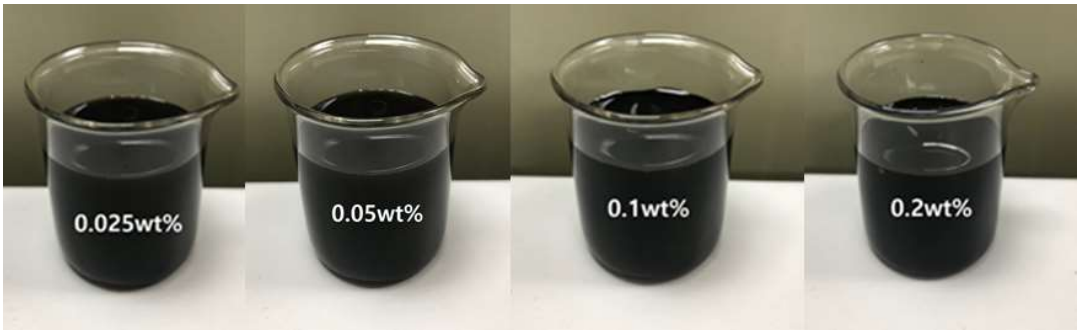

(a) MWCNT nanofluids

(b) Fe_3O_4 nanofluids

(c) MWCNT/Fe_3O_4 hybrid nanofluids

Fig. 2.5 Pictures of (a) MWCNT nanofluids, (b) Fe_3O_4 nanofluids, and (c) MWCNT/Fe_3O_4 hybrid nanofluids

2.3 Thermal conductivity measurement of MWCNT, Fe_3O_4, and MWCNT/Fe_3O_4 hybrid nanofluids

The transient how wire technique was used in this analysis to calculate thermal conductivity nanofluids. The hot wire method is to measure the thermal conductivity of working fluids using equipment, which is easily accessible in a physical laboratory. The thermal conductivity of nanofluids depends on many factors such as particle volume fraction, particle material, particle size, particle shape, base fluid material, and temperature. In this experiment, the thermal conductivity was measured by the thermal conductivity analyzer (KD2 Pro) manufactured by Decagon Devices Inc. This measuring device is a handheld device used to measure thermal properties of working fluid. There are several sensors available for use that operators can insert into any material. KD2 Pro consists of single needle with a length and diameter of 60 and 1.3 mm. The thermal constant bath (VS-190CS), thermal conductivity measurement device (KD2 Pro), double glass beaker and temperature sensor were used to measure the thermal conductivity of nanofluid. The thermal constant bath with 20 L capacity was used to control the temperature of working fluid constantly, and the temperature sensor (K-type) and test section of laboratory glass filled with working fluid which covered by a double glass beaker. The double glass beaker should be used to prevent against temperature disturbance. Double glass beaker was insulated by pink foam. The experimental and schematic components are shown in Fig. 2.6. Before the test, the measuring equipments were checked with water for calibration process. After, thermal conductivity of MWCNT, Fe_3O_4, and

MWCNT/Fe_3O_4 hybrid nanofluids were measured at the temperature of 25°C.

(a) KD2 Pro (b) Thermal constant bath

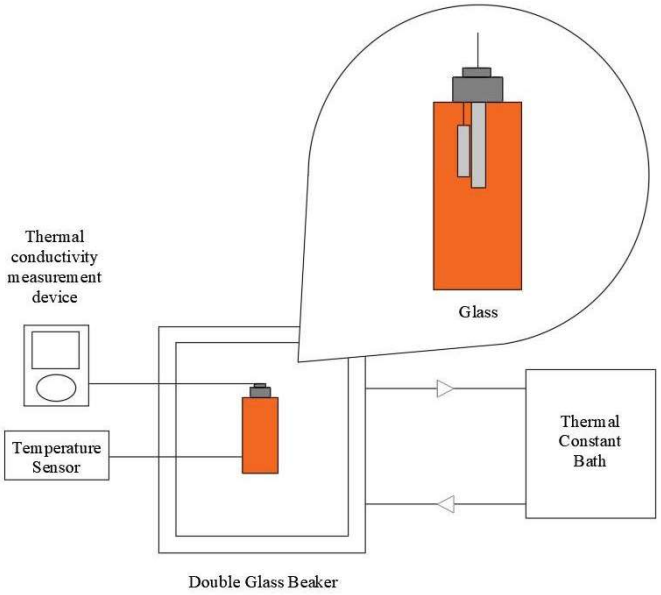

(c) Schematic of thermal conductivity measurement

Fig. 2.6 Thermal conductivity measurement devices of (a) KD2 Pro, (b) Thermal constant bath (c) Schematic of thermal conductivity measurement

2.4 Experimental setup and equipments of convective heat transfer

The convective heat transfer equipment consists of the test section, DC power supply, pressure transmitter, brazed plate heat exchanger, micro gear pump, storage tank, thermocouples, and data acquisition system. Fig. 2.7 shows the schematic and pictures of the experimental setup for measuring performance of convective heat transfer. The test section had a stainless steel tube of 1.5 m with inner and outer diameter of 3.7 and 6.3 mm, respectively. The thermocouples are installed on the tube at the distance of x=300 mm from the entrance of the test section. The low temperature water bath provided for setting the inlet temperature to the required level. Therefore, peroxide-cured silicone tubes were installed on the inlet and outlet of the test section, which was insulated with rubber foam insulation material. Table 2.3 shows the experiment conditions of convective heat transfer.

Table 2.3 Experiment conditions of convective heat transfer

Items	Specifications
Test section	Stainless steel
Tube length (mm)	1500
Inner diameter (mm)	3.7
Outer diameter (mm)	6.3

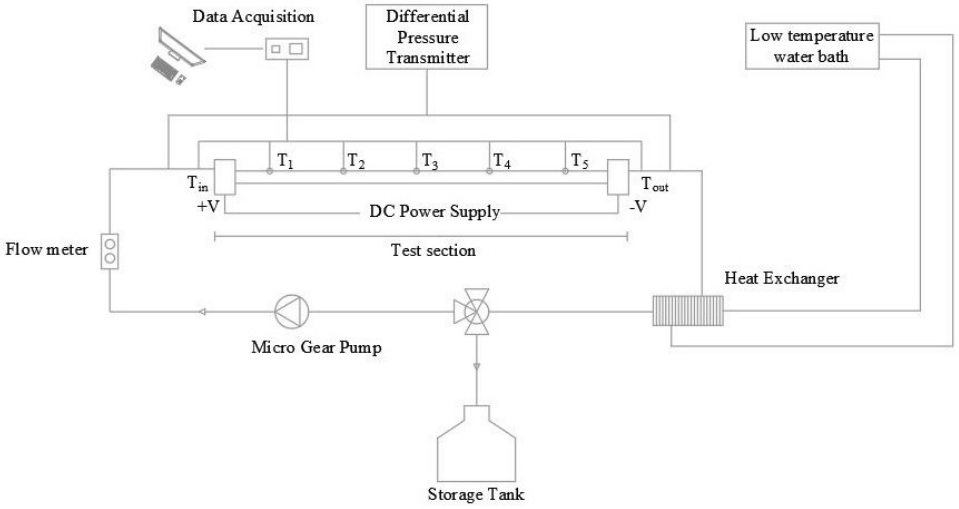

(a) Schematic of convective heat transfer experiment setup

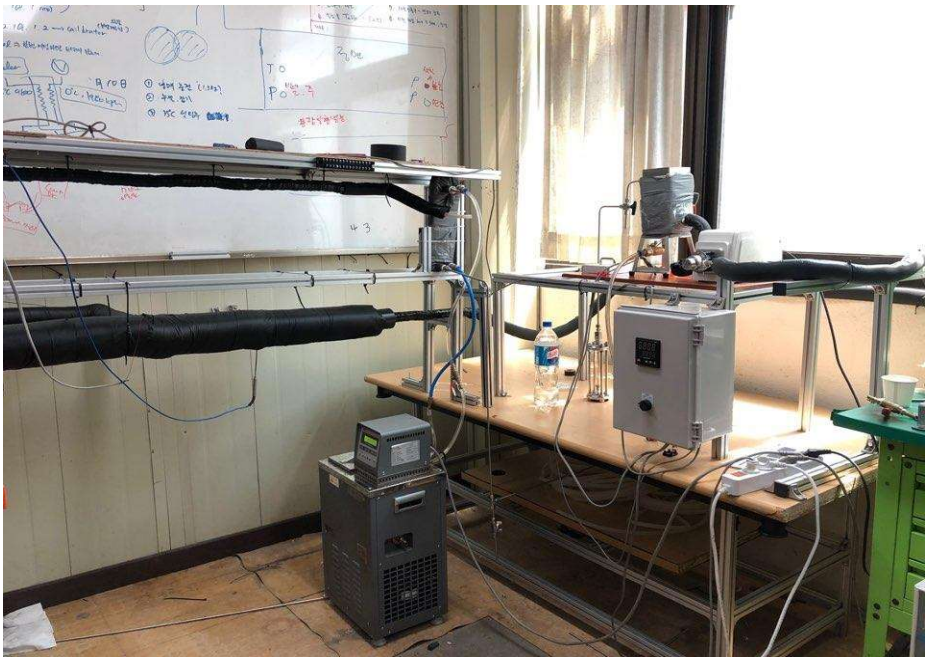

(b) Picture of experimental setup [part 1]

(c) Picture of experiment setup [part 2]

Fig. 2.7. Experimental setup of convective heat transfer (a) Schematic of convective heat transfer experimental setup (b) Picture of experimental setup [part 1] (c) Picture of experimental setup [part 2]

A. Brazed plate heat exchanger

A brazed plate heat exchanger is the type of heat exchanger that uses welded metal plates to transfer heat between two liquids. In this research, the brazed plate heat exchanger (B3-030-10-3.0-HQ) was used which has a cost effective component for conventional evaporators, condensers, commercial and industrial refrigeration, cooling and air conditioning applications. The advantages of brazed plate heat exchanger are less space, wide range of sizes, cooling capacity, high heat transfer, and capable for high viscosity fluids. Fig. 2.8 and Table 2.4 show the image and specifications of the brazed plate heat exchanger.

Fig. 2.8 Brazed plate heat exchanger (B3-030-10-3.0-HQ)

Table 2.4 Specifications of brazed plate heat exchanger

Items	Specifications
Model	B3-030-10-3.0-HQ
Temperature range (°C)	-196/+200
Pressure range (bar)	-1/30

B. Micro gear pump

The micro gear pump controls the low viscosity of working fluids, solvents, and liquid gases. The fluids containing solids are not suitable for micro gear pumps because nanoparticles are nano-sized solids dispersed in the conventional fluid. For this reason, nanofluid dispersion stability will be higher and there will be no sedimentation for each experiment. The advantages of the micro gear pump are high dosing accuracy, high efficiency, low pulsation promotion, low costs, high capability, and low maintenance. Fig. 2.9 and Table 2.5 show the image and specifications of the micro gear pump.

Fig. 2.9 Micro gear pump (WT3000-1FA)

Table 2.5 Specifications of micro gear pump

Items	Specifications
Model	WT3000-1FA
Flow rate (ml/min)	85.7 to 2571.4
Speed (rpm)	300-3000
Accuracy (%)	±1.0
Diameter of particle in liquid (μm)	10
Temperature (°C)	-45 to 120

C. Power supply

The power supply is an electrical device which supplies electrical power to the test section. The power supplies include a power input connection that produces energy from the source in the electrical current, and power output connections that provide experimental current. For this research, DC power supply (DSP-2005) is designed to supply energy at voltage and current. The output of the DC power supply was dependents on the input of the voltage reduction transformer and matched the output of the current required by the load. As a consequence, the output of the voltage decreases with an increase in the outlet of current. Fig. 2.10 and Table 2.6 show the image and specifications of the DC power supply.

Fig. 2.10 DC power supply (DSP-2005)

Table 2.6 Specifications of DC power supply

Items	Specifications
Model	DSP-2005
Normal capacity (kW)	1
Maximum voltage (V)	200
Maximum current (A)	5

D. Low temperature water bath

Low temperature water bath consists of a container filled with heated water. It is used to perform experiment in water at a constant temperature for a long period of time. Low temperature water bath is the heated bath circulators for water, oil, liquid. The advantages of low temperature water bath are cost efficient, high quality and easy to circulate for the inlet of test section. Fig. 2.11 and Table 2.7 show the image and specifications of low temperature water bath.

Fig. 2.11 Low temperature water bath (RBC-08)

Table 2.7 Specifications of DC power supply

Items	Specifications
Model	RBC-08
Bath capacity (Liter)	8
Heater capacity (W)	1500
Temperature range (°C)	-20 to 95
Temperature accuracy	±0.5

Measuring equipment used for the measurement of physical and electrical quantities is defined as the measuring equipments. Measuring equipments of convective heat transfer are devices for measuring a mass flow rate, temperature,

pressure, and data acquisition system in convective heat transfer. In this step, a set of measuring devices for convective heat transfer are presented.

E. Precision balance

The measurement of mass of working fluid is possible using an electronic weighing scale (precision balance of FX-300i) and the proper signal processing. The liquid flow-weighing system consists of the flow control valve, pipe or nozzle, collection tank, and precision balancer. The mass flow rate measured by weighing the quantity of working fluid during certain measuring time. Fig. 2.12 shows the liquid flow weighing measurement of mass flow rate and device of precision balance. In addition, the specifications of precision balance is shown in Table 2.8.

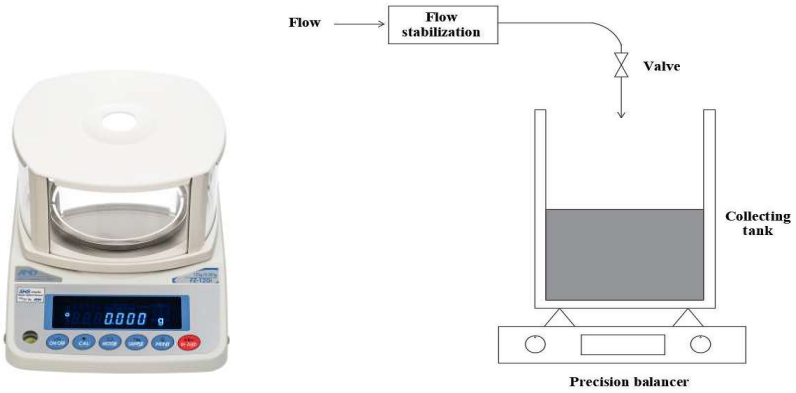

Fig. 2.12 The mass flow rate measurement of (a) Precision Balance (FX-300i) (b) The liquid flow-weighing measurement

Table 2.8 Specifications of precision balance

Items	Specifications
Model	FX-300i
Maximum capacity (gram)	320

F. T-type thermocouple

The thermocouple is the sensor to measure temperature of test object. T-type thermocouple consists of two wires of different material connected at the end. One loop is located at the point of measuring temperature, and the other loop is located at a constant lower temperature. That temperature difference causes the development of an electromotive force which is approximately proportional to the difference between the temperatures of the two loops. The T-type thermocouple is a noticeable stable and is widely used in low temperature applications. Fig. 2.13 and Table 2.9 show the image and specifications of T-type thermocouple of this study.

Fig. 2.13 T-type thermocouples

Table 2.9 Specifications of T-type thermocouple

Items	Specifications
Model	T-Type thermocouple
Temperature range (°C)	-200 to 300
Accuracy (°C)	±1.0

G. Pressure transmitter

The pressure transmitter is used to measure the pressure of working fluid in the test section of this experiment. The pressure drop between the inlet and the outlet of tube was measured with the pressure transmitter. The output of working fluid is transmitted to a control system. Accuration and stabilization process of measurement equipment to guarantee for the safe, stable, and useful operation of the experiment. Fig. 2.14 and Table 2.10 show picture and specifications of T-type thermocouple.

Fig. 2.14 Pressure transmitter (2301005PD2F11BC)

Table 2.10 Specifications of pressure transmitter

Items	Specifications
Model	2301005PD2F11BC
Range (PSID)	0-5
Output (mA)	4-20

H. Data acquisition system

The data acquisition system is the measurment of the physical parameters and converting to the numerical values of results that can be operate with computer. Data acquisition system starts with the same time of physical property to be measured, to include temperature, pressure, light intensity, fluid force and mass flow. This system consists of a DAQ hardware, sensor, and signal condition hardware. In this experiment, the data acquisition system (MX100) which is designed to operate with PCs is used. Fig. 2.15 and Table 2.11 show picture and specifications of the data acquisition system.

Fig. 2.15 Data acquisition system (MX100)

Table 2.11 Specifications of data acquisition system

Items	Specifications
Model	MX100
Number of inputs	10
Measurement interval (ms)	100
Operating temperature range (°C)	0 to 50
Rated power supply voltage (VDC)	12 to 28

2.5 Operating condition and method of experiment

An experimental setup was designed to examine the convective heat transfer characteristics of MWCNT, Fe_3O_4, and MWCNT/Fe_3O_4 hybrid nanofluids flowing through a tube under constant heat flux boundary conditions. The nanofluids with different weight concentrations based into the base fluid of EG/Water=20:80 are pumped in the test section using a peristaltic pump with a maximum flow rate of 85.7-2571.4 ml/min. Subsequently, the outer test section was winded by a nichrome heating wire. The working fluid is uniformly heated with the nichrome wire. The heat was supplied by DC power supply with a maximum output of 1 kW. The power was measured by a voltmeter and an amperemeter with accuracy of 0.01 V and 0.001 A. The heat loss was estimated to be less than 10%. After, the fluid was cooled down to inlet temperature by recirculating low temperature water bath (DS-RBC-08) directed to the 8 liter vessel. Thermocouples attached on the wall of test section at regular intervals to determine the wall temperature. The temperatures were measured by five thermocouples of T-type with an accuracy of 0.1°C Two thermocouples are placed into the flow at the inlet and outlet of the test section to measure bulk temperatures of nanofluids. During experiment, the inlet and outlet temperatures of nanofluid and the wall temperature were measured. Each measurement was repeated three times. The operating conditions are shown in Table 2.12

Table 2.12 Operating conditions of experiment

Items	Specifications
Working fluid	EG/Water (20:80), MWCNT, Fe_3O_4, and MWCNT/Fe_3O_4 hybrid nanofluid
Reynolds numbers	1000, 1200, 1400, 1600
Inlet temperature (°C)	25
Power supply (W)	100
Mass flow rate (kg/s)	0.005-0.009
Velocity (m/s)	0.381-0.715

2.6 Data reduction

The density and specific heat of single nanofluid were estimated based on the Pak and Cho [39] equation, which are calculated by Eqs. (2,3)

$$\rho_{nf} = (1-\phi)\rho_{bf} + \phi \times \rho_p \tag{2}$$

$$C_{nf} = (1-\phi)C_{bf} + \phi \times C_p \tag{3}$$

Where ϕ is the weight concentration of nanofluid, ρ_{bf}, ρ_{nf} and ρ_p are the density of the base fluid, nanofluid and nanoparticle, C_{bf}, C_{nf} and C_p are the specific heat of base fluid, nanofluid, and nanoparticle. For the hybrid nanofluid, the density and specific heat were based on the equations, which are calculated by Eqs. (4,5)

$$\rho_{CNT+Fe_3O_4} = \frac{\rho_{CNT} \times w_{CNT} + \rho_{Fe_3O_4} \times w_{Fe_3O_4}}{w_{CNT} + w_{Fe_3O_4}} \tag{4}$$

$$C_{CNT+Fe_3O_4} = \frac{C_{CNT} \times w_{CNT} + C_{Fe_3O_4} \times w_{Fe_3O_4}}{w_{CNT} + w_{Fe_3O_4}} \tag{5}$$

Where w_{CNT} and $w_{Fe_3O_4}$ are the weight of the MWCNT and Fe_3O_4 nanofluids, C_{CNT} and $C_{Fe_3O_4}$ are the specific heat of MWCNT and Fe_3O_4 nanofluids. The amount of energy supplied to the test section and the absorbed heat by the working fluid which are calculated by the Eqs. (6,7)

$$P = V \times I \tag{6}$$

$$Q = m \times C \times (T_0 - T_i) \tag{7}$$

Where V is the voltage, I is the current of power supply, m and C are the mass flow rate and specific heat of working fluid, T_o and T_i are the outlet and inlet of temperature of test section. The local heat of convective heat transfer coefficients along the axial distance of test section are calculated by Eq. (8)

$$h = \frac{Q}{A(t_w - t_b)} \tag{8}$$

Where A is the area of test section, t_w and t_b are the temperature of wall and bulk. The area, wall and bulk temperatures are calculated by

$A = \pi DL$, $t_w = \frac{\sum T}{5}$, and $t_b = \frac{T_o + T_i}{2}$, respectively.

The Nusselt number is the directly proportional to the convective heat transfer coefficient which increases with the Nusselt number. The Nusselt number is calculated by Eq. (9)

$$Nu = \frac{h \times D}{k} \tag{9}$$

Where D is the inlet diameter of test section, k is the thermal conductivity of nanofluid. The friction factor is the related to the pressure drop which is measured across the test section under flow condition is used to determine the friction factor which is calculated by Eq. (10)

$$f = \frac{\triangle P}{\left(\frac{L}{D}\right)\left(\frac{\rho v^2}{2}\right)} \tag{10}$$

Where L is the length of the test section, ρ is the density of the working fluid, v is the velocity of the working fluid at Reynolds number.

2.7 Uncertainty analysis

The calculation of the experiment error in the measurement of the experimental analysis is based on the method used by Beckwith et al. [40]. The uncertainties of Reynolds number, heat flux, convective heat transfer coefficient, and Nusselt number are estimated with Eqs. (13), (14), (15), and (16). The uncertainties of measuring device and experimental result are presented in Tables 2.13 and 2.14.

$$\frac{U_{Re}}{Re} = \sqrt{\left(\frac{U_{\dot{m}}}{\dot{m}}\right)^2 + \left(\frac{U_{\mu}}{\mu}\right)^2} \tag{13}$$

$$\frac{U_q}{q} = \sqrt{\left(\frac{2U_{\nu}}{V}\right)^2 + \left(\frac{U_R}{R}\right)^2} \tag{14}$$

$$\frac{U_h}{h} = \sqrt{\left(\frac{U_q}{q}\right)^2 + \left(\frac{U_{T_w - T_b}}{T_w - T_b}\right)^2} \tag{15}$$

$$\frac{U_N}{N} = \sqrt{\left(\frac{U_h}{h}\right)^2 + \left(\frac{U_K}{K}\right)^2} \tag{16}$$

Table 2.13 The uncertainties of measuring devices

Parameter	Instrument	Uncertainty (%)
Thermocouple (K)	Calibrated T-type thermocouple	0.1
Voltage (V)	DC power supply	0.1
Current (A)	DC power supply	0.01
Time (s)	Time taken	0.01

Table 2.14 The uncertainty analysis for the experimental results

Parameter	Uncertainty (%)
Reynolds number, Re	0.10
Heat flux, q	0.2126
Convective heat transfer coefficient, h	0.2332
Nusselt number, Nu	0.2538

Ⅲ. Results and discussion

3.1 Validation of the experimental result

An experimental setup was validated by using Shah equation [41] for the convective heat transfer experiment. The experiment was conducted with pure water in the circular tube according to Reynolds number between 1000 and 1600. There investigations were compared with our experimental results for pure water along the axial distance of the test section. They reported this validation can be calculated by Eqs. (11,12)

$$Nu = \begin{cases} 1.953 \times (x_L^*)^{-1/3} & x_L^* \le 0.03 \\ 4.364 + 0.0722/x_L^* & x_L^* > 0.03 \end{cases} \tag{11}$$

$$x_L^* = \frac{L}{\mathrm{Pr} \times Re \times D} \tag{12}$$

Nusselt number calculation is separated into two sections where x_L^* is the reference parameter. It can be seen from Fig. 3.1 which results corresponded greatly to our test results of Nusselt number along the axial distance of the test section. It is seen that there is a strong agreement with effects of pure water.

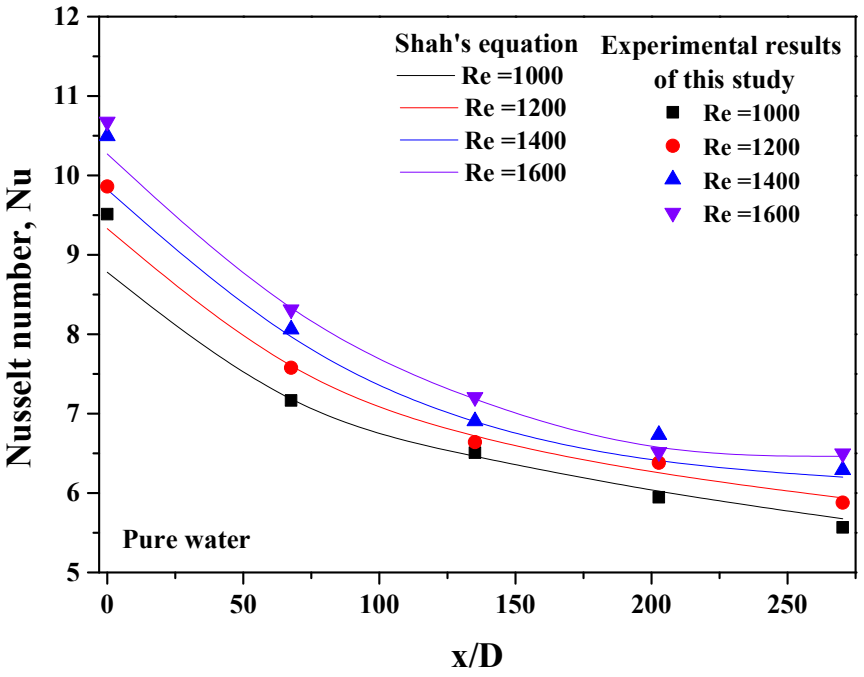

Fig. 3.1 Comparison of the measured Nusselt number with the theoretical correlation of Shah equation for pure water

3.2 Thermal conductivity of MWCNT, Fe_3O_4, and MWCNT/Fe_3O_4 hybrid nanofluids

Fig. 3.2 shows the variation of thermal conductivity of MWCNT, Fe_3O_4, MWCNT/Fe_3O_4 hybrid nanofluids at various concentrations. In this experiment, all concentrations of MWCNT nanofluids were higher than that of other nanofluids. The increment of weight concentration leads to increase the thermal conductivity of MWCNT nanofluids. The maximum thermal conductivity of MWCNT nanofluid was 0.537 W/mK, which was observed at weight concentration and temperature of 0.2wt% and 25°C, respectively. Improving thermal conductivity can be explained by the increased interactions of nanoparticles in the base fluid (EG/Water=20:80). This interaction causes the diffusion of heat in nanofluids, which is called Brownian motion. Compared to the thermal conductivity of base fluid, the maximum thermal conductivity improvement of MWCNT nanofluid was 6.3% which was observed at the weight concentration of 0.2wt% and the temperature of 25°C compared to the base fluid. Moreover, the thermal conductivity of MWCNT/Fe_3O_4 hybrid nanofluid was significantly improved compared to that of Fe_3O_4 nanofluid. The maximum thermal conductivity of MWCNT/Fe_3O_4 hybrid nanofluid was 0.531 W/mK, which was observed at 0.2wt% MWCNT/Fe_3O_4 hybrid nanofluid and the temperature of 25°C, respectively. This improvement is due to the effect of adding MWCNT nanoparticles. Since, the weight mixing ratio of MWCNT/Fe_3O_4 hybrid nanofluid was arranged at 1:1, the number of MWCNT nanoparticles in MWCNT/Fe_3O_4 hybrid nanofluids were greater than that of Fe_3O_4 nanoparticles because of their density differences affected to the MWCNT/Fe_3O_4 hybrid nanofluid. Yarmand et al.

[42] reported that this percolation effect caused by a high concentration of nanofluid, reducing the distance between nanoparticles and increasing lattice vibrational frequency. With increasing weight concentration the nanoparticle distance decreases. This is due to the effect of percolation. It can be observed that the thermal conductivity of nanofluids increases with an increase in weight concentrations. The decrement of the distance between nanoparticles improves the thermal conductivity of nanofluids.

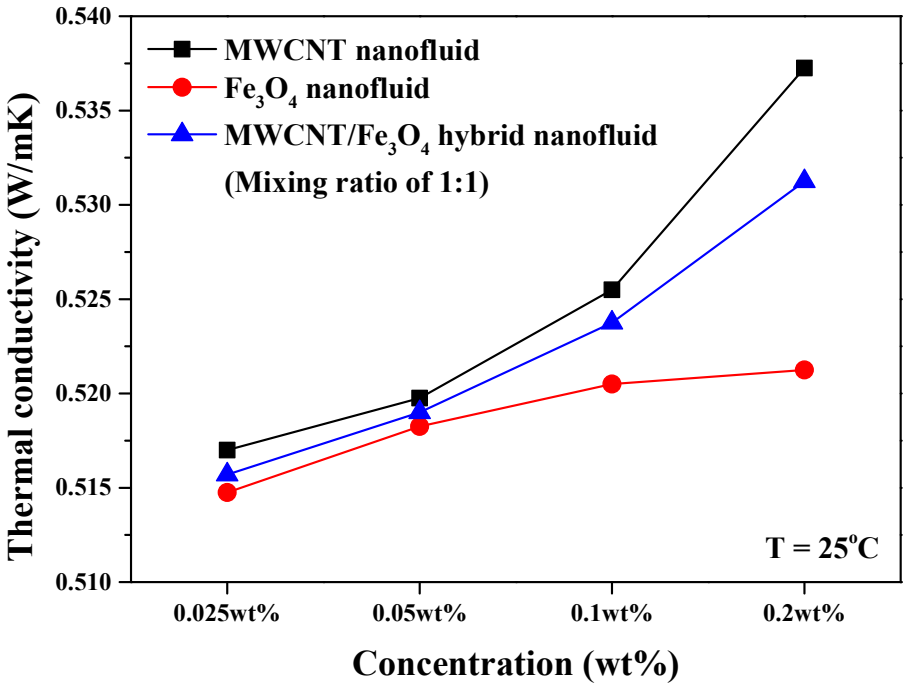

Fig. 3.2 Variation of the thermal conductivity at the temperature of 25°C under different weight concentration of nanofluids

3.3 Convective heat transfer of MWCNT, Fe_3O_4, and MWCNT/Fe_3O_4 hybrid nanofluids

Fig. 3.3 shows the variation of the convective heat transfer coefficient of MWCNT nanofluid with varying weight concentrations under different Reynolds numbers. When the concentration of the MWCNT nanofluid increased from 0.025wt% to 0.2wt%, the convective heat transfer coefficient increased from 1892.1 to 1990 W/m^2K, with 4.8% to 10.2% increase in convective heat transfer coefficient compared to that of the base fluid. It is clearly seen that the maximum improvement of the convective heat transfer coefficient was observed at 0.2wt% MWCNT nanofluid, which was 10.2% higher than the base fluid at Reynolds number of 1600. The convective heat transfer coefficient improvement of MWCNT nanofluid was 1892.1, 1899.4, and 1983.8 W/m^2K, respectively, which were 4.8%, 5.2%, and 9.9% at the weight concentrations of 0.025wt%, 0.05wt%, and 0.1wt%, compared with that of the base fluid. Fig. 3.4 presents the variation of the Nusselt number of MWCNT nanofluid with different weight concentrations and Reynolds numbers. The Nusselt number of MWCNT nanofluid concentrations of 0.025wt%, 0.05wt%, 0.1wt% and 0.2wt%, were 12.22, 12.27, 12.82 and 12.86, respectively, which were higher than the base fluid. The Nusselt number increased by increasing the Reynolds number at the same weight concentration of nanofluid. The improvement of the Nusselt number is directly related to the convective heat transfer coefficient with an increase in weight concentration. By increasing the Reynolds number with the Nusselt number increases the convective heat transfer coefficient.

Figs. 3.5 and 3.6 represent the variation of convective heat transfer coefficient and Nusselt number of Fe_3O_4 nanofluid at different weight concentrations and Reynolds numbers. The convective heat transfer coefficients of Fe_3O_4 nanofluid ranged from 1870.1 to 1963.5 W/m^{2}K for Reynolds number of 1600. The maximum increase in the convective heat transfer coefficient was 1963.5 W/m^{2}K at the 0.2wt% Fe_3O_4 nanofluid, which was 8.7% higher than the base fluid at Reynolds number of 1600. The improvement of convective heat transfer coefficient of Fe_3O_4 nanofluid was 1870.1, 1889.4, and 1951.8 W/m^{2}K, respectively which were 3.6%, 4.6%, and 8.1% at the weight concentrations of 0.025wt%, 0.05wt% and, 0.1wt%, compared to those of the base fluid. The Nusselt number of Fe_3O_4 nanofluid was 12.85, 12.37, 12.78 and 13.12, with a weight concentrations of 0.025wt%, 0.05wt%, 0.1wt% and 0.2wt%, respectively. Figs. 3.7 and 3.8 show the variation of convective heat transfer coefficient and Nusselt number of MWCNT/Fe_3O_4 hybrid nanofluid at various weight concentrations and Reynolds numbers. The convective heat transfer coefficients of MWCNT/Fe_3O_4 hybrid nanofluid ranged from 1914.3 to 1988.4 W/m^{2}K, with 6% to 12.4% higher than the base fluid. The maximum improvement in the convective heat transfer coefficient was seen at 0.1wt% MWCNT/Fe_3O_4 hybrid nanofluid, which was 12.4% higher than that of base fluid at Reynolds number of 1600. The convective heat transfer coefficient improvement of MWCNT/Fe_3O_4 hybrid nanofluid was 1914.3, 1958.5, and 1988.4 W/m^{2}K, respectively, which were 6%, 8.5%, and 10.1% at weight concentration of 0.025wt%, 0.05wt%, and 0.2wt%, respectively, compared to those of the base fluid. As shown in Fig. 3.8, the Nusselt number of MWCNT/Fe_3O_4 hybrid nanofluid was 12.37, 12.78, 13.12 and 12.85, with a weight concentration of 0.025wt%, 0.05wt%, 0.1wt% and 0.2wt%, respectively. The Nusselt number

increases with an increase in nanofluid weight concentrations and also increases with increase Reynolds number ranging from 1000 to 1600. The improvement of the convective heat transfer coefficient of MWCNT/Fe_3O_4 hybrid nanofluid is restricted by the thermo-physical properties and the random movement of the nanoparticles with the different Reynolds numbers at a high weight concentration of 0.2wt%. It can be assumed that extra thermal resistance on the inner surface of the test section was caused by the agglomerated Fe_3O_4 nanoparticles that coated the inner surface of the test section at high Fe_3O_4 nanofluid concentrations. Also, the viscosity of the Fe_3O_4 nanofluid increased with the increase of nanofluid concentration.

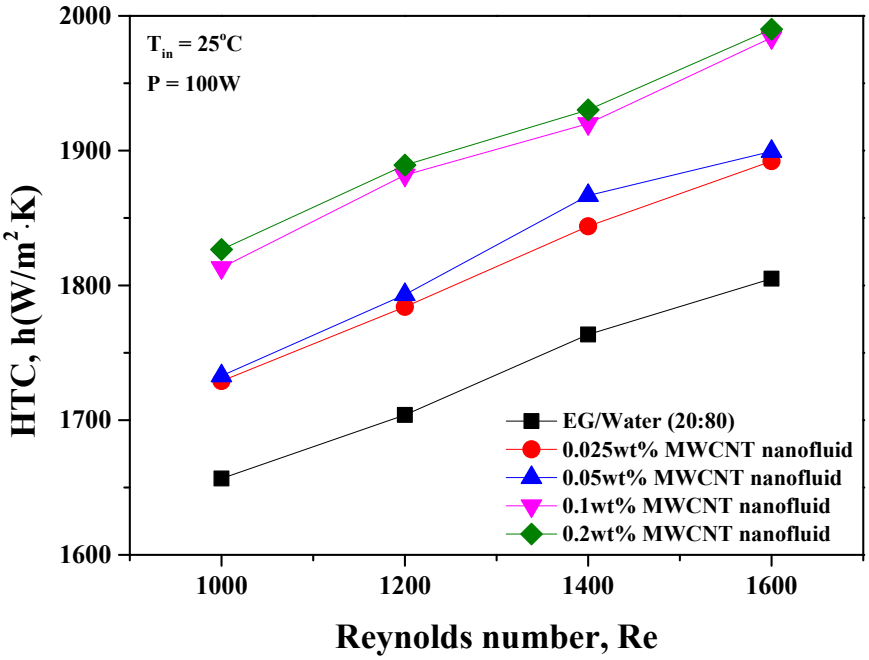

Fig. 3.3 Variation of the convective heat transfer coefficient with MWCNT nanofluids according to Reynolds numbers

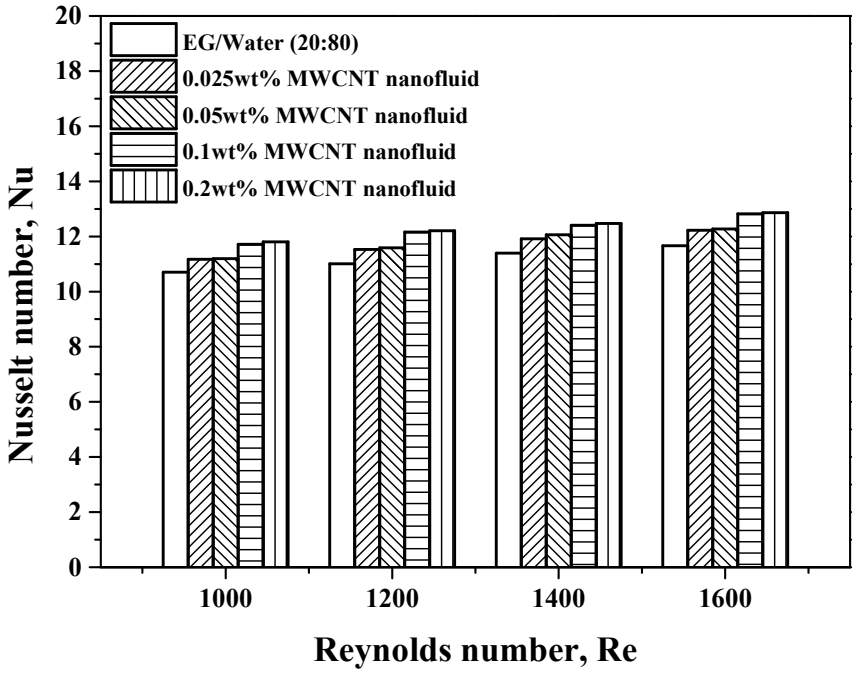

Fig. 3.4 Nusselt number of MWCNT nanofluids according to the weight concentrations and Reynolds numbers

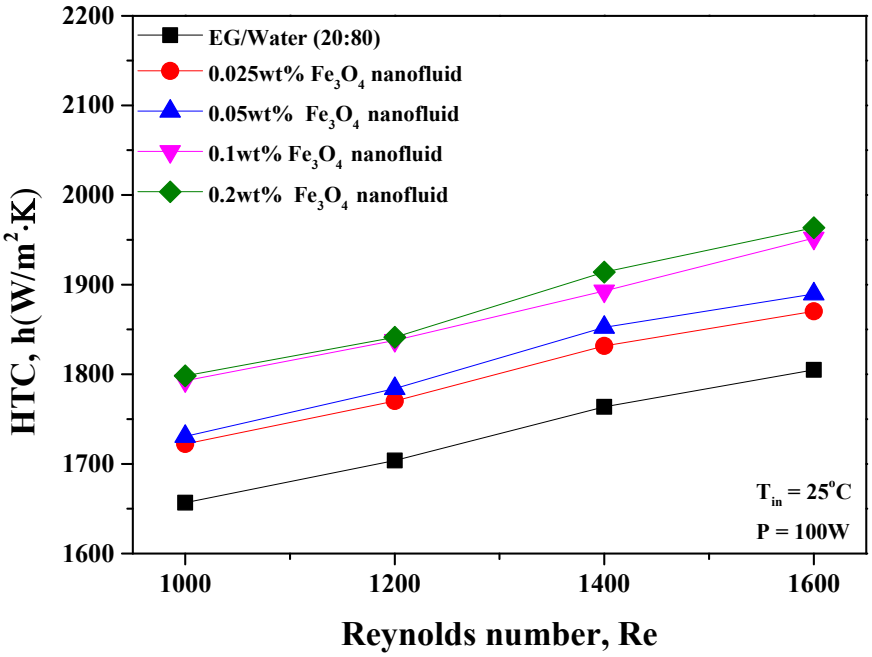

Fig. 3.5 Variation of the convective heat transfer coefficient with Fe_3O_4 nanofluids according to Reynolds numbers

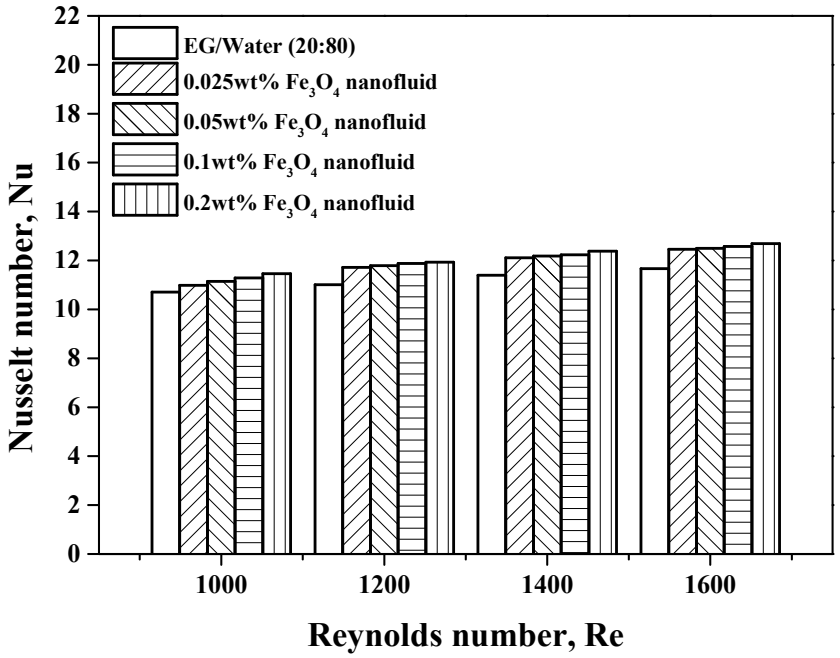

Fig. 3.6 Nusselt number of Fe_3O_4 nanofluids according to the weight concentrations and Reynolds numbers

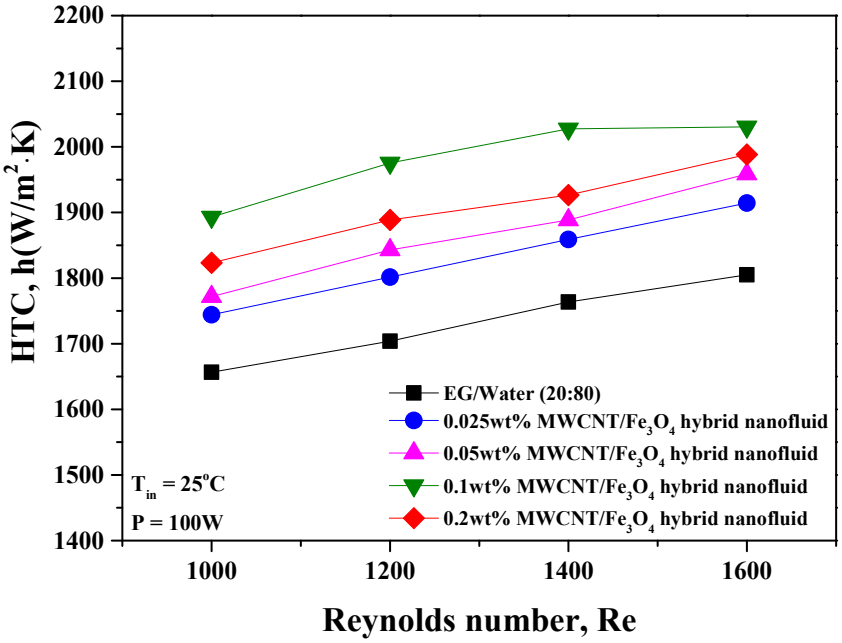

Fig. 3.7 Variation of the convective heat transfer coefficient with MWCNT/Fe_3O_4 hybrid nanofluids according to Reynolds numbers

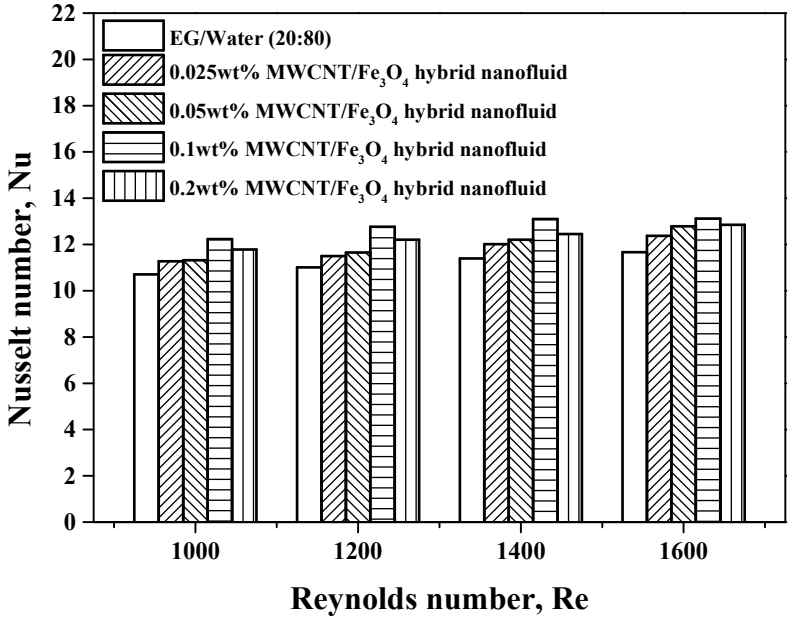

Fig. 3.8 Nusselt number of MWCNT/Fe_3O_4 hybrid nanofluids according to the weight concentrations and Reynolds numbers

3.4 Pressure drop of MWCNT, Fe_3O_4, and MWCNT/Fe_3O_4 hybrid nanofluids

Fig. 3.9 shows the variation of pressure drop of nanofluids according to the weight concentrations and Reynolds numbers. The pressure drop of MWCNT nanofluid ranged from 2.96 to 3.24 kPa according to Reynolds number. The maximum value of the pressure drop was 3.24 kPa at the highest weight concentration of 0.2wt% MWCNT nanofluid, which increased by 49.6% compared to the base fluid. The pressure drop of 0.025wt%, 0.05wt%, and 0.1wt% MWCNT nanofluids was 2.96, 3.09, and 3.12 kPa, with 36.7%, 42.6%, and 44.1%, respectively, higher than the base fluid. As can be seen in figures, as nanoparticle concentration increases, the pressure drop of nanofluid increases. Compared with base fluid, no significant enhancement in pressure drop for various nanofluids was found in the same Reynolds number. Fig. 3.10 shows the friction factor of MWCNT nanofluids according to the nanoparticle weight concentrations and Reynolds numbers. When the concentration of MWCNT increased from 0.025wt% to 0.2wt%, the friction factor increased from 0.0329 to 0.0342, with 26.2% to 31.3% increase in friction factor compared to that of the base fluid. The friction factor increase of 0.2wt% of MWCNT nanofluid was 31.3% higher than the base fluid. As Reynolds numbers were increased, friction factors decreased for all nanofluids. It can be concluded that the pressure drop of base fluid was higher than that of all nanofluids at the Reynolds number of 1600.

Fig 3.11 shows the variation of pressure drop with different weight concentrations of Fe_3O_4 nanofluid according to Reynolds numbers. The pressure

drop increment of Fe_3O_4 nanofluid was 3, 3.11, and 3.19 kPa, respectively, which were 38.4%, 43.3% and 47% at the weight concentrations of 0.025wt%, 0.05wt% and 0.1wt%, compared with those of the base fluid. The maximum pressure drop was 3.37 kPa at the weight concentration of 0.2wt% Fe_3O_4 nanofluid, which was increased by 55.2% compared to the base fluid at Reynolds number of 1600. The friction factor of 0.025wt%, 0.05wt% and 0.1wt% Fe_3O_4 nanofluids was 0.0298, 0.0310 and 0.0320, with 14.5%, 19.1% and 22.8%, respectively, higher than the base fluid. In Fig, 3.12, the increment of friction factor for 0.2wt% of Fe_3O_4 nanofluid was 0.0355 which improves 36% higher than the base fluid.

Fig. 3.13 shows the variation of pressure drop for different weight concentrations of MWCNT/Fe_3O_4 hybrid nanofluids according to Reynolds numbers. The pressure drop of MWCNT/Fe_3O_4 hybrid nanofluid was 3.1, 3.16, and 3.29 kPa, which were 43%, 46%, and 51.9% at the weight concentrations of 0.025wt%, 0.05wt% and 0.1wt%, compared with the base fluid. The maximum pressure drop was seen at the weight concentration of 0.2wt% MWCNT/Fe_3O_4 hybrid nanofluid was 3.52 kPa, which increased up to approximately 62.4% at Reynolds number of 1600, compared to the base fluid. Fig. 3.14 shows the friction factor of MWCNT/Fe_3O_4 hybrid nanofluids according to the weight concentration and Reynolds number. The friction factor of 0.025wt%, 0.05wt% and 0.1wt% MWCNT/Fe_3O_4 hybrid nanofluids was 0.0331, 0.0339 and 0.0355, with 26.9%, 30.2% and 36.3%, respectively, higher than the base fluid. The increment of the friction factor was 0.0407 for 0.2wt% MWCNT/Fe_3O_4 hybrid nanofluid which improves 56% higher than the base fluid. The friction factor for all concentrations decreased with an increasing Reynolds number. Generally, the friction factor increases with the increasing concentration of nanoparticles. It can be concluded that the

viscosity of nanofluids increases proportionally with the concentration, which increases the viscous sublayer and increases the friction factor.

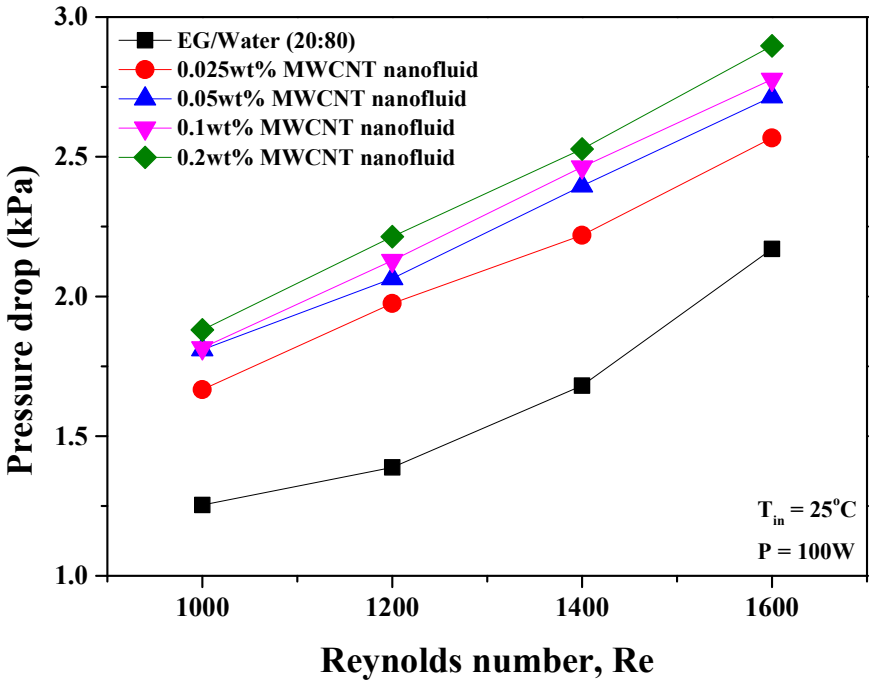

Fig. 3.9 Variation of pressure drop with MWCNT nanofluids according to Reynolds numbers

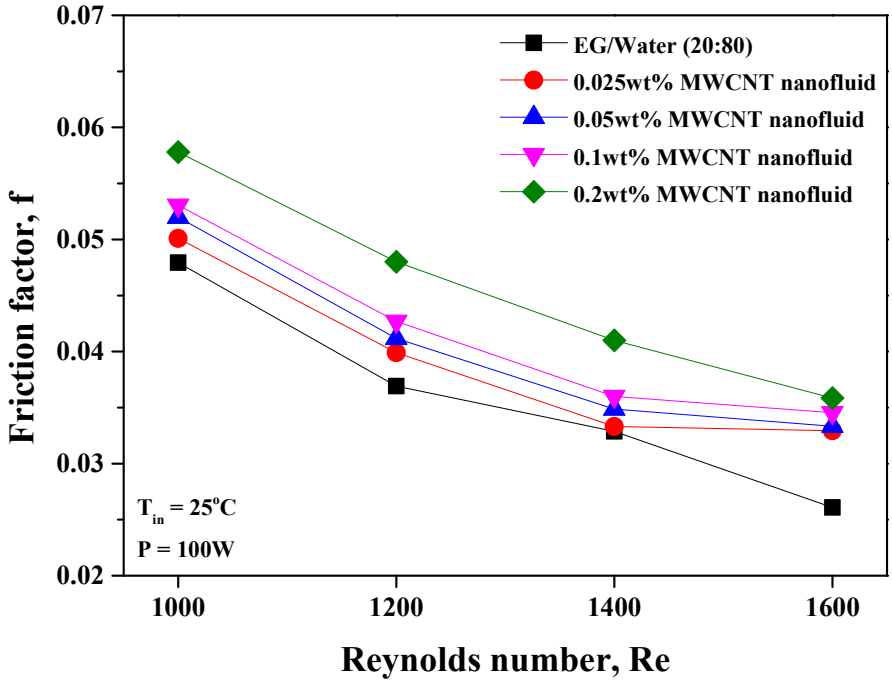

Fig. 3.10 Variation of friction factor with MWCNT nanofluids according to the weight concentrations and Reynolds numbers

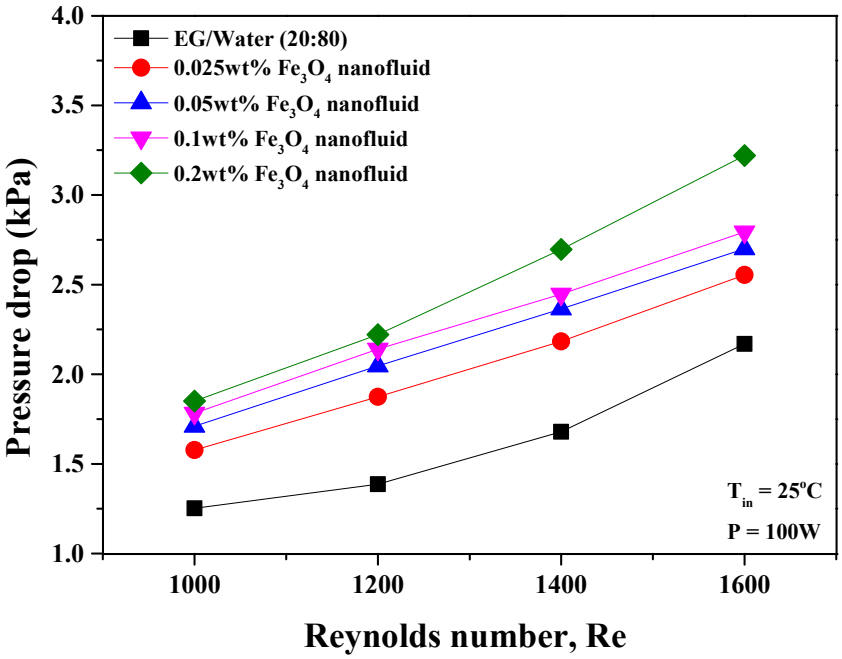

Fig. 3.11 Variation of pressure drop with Fe_3O_4 nanofluids according to Reynolds numbers

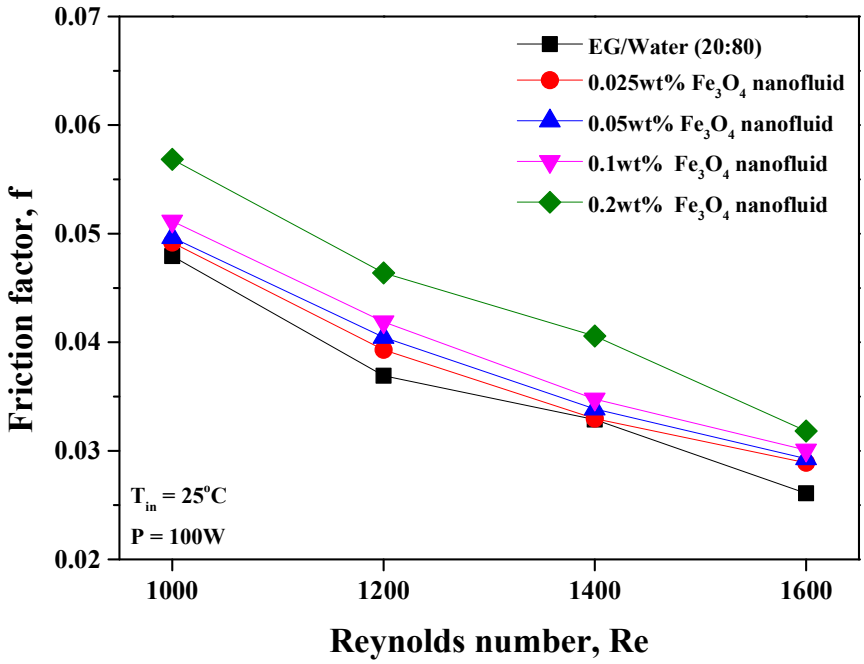

Fig. 3.12 Variation of friction factor with Fe_3O_4 nanofluids according to the weight concentrations and Reynolds numbers

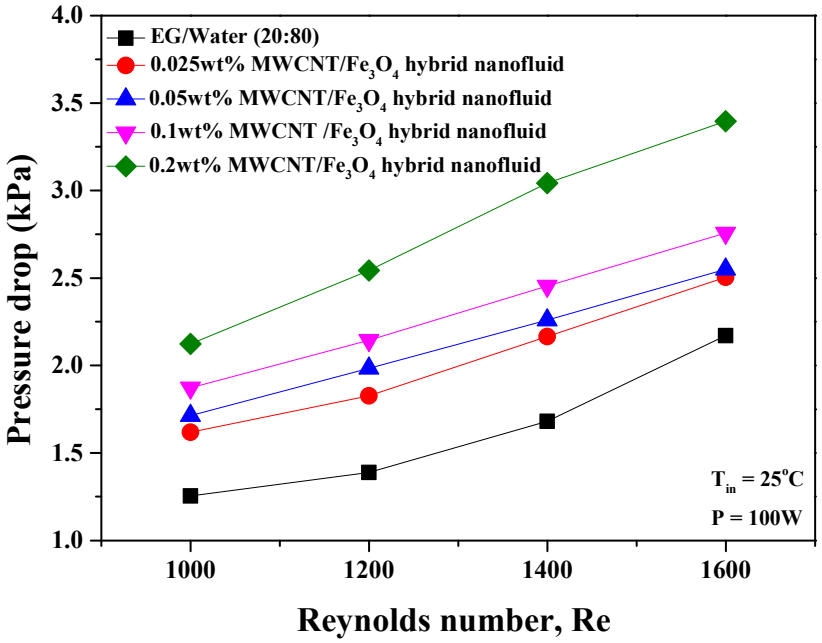

Fig. 3.13 Variation of pressure drop with MWCNT/Fe_3O_4 hybrid nanofluids according to Reynolds numbers

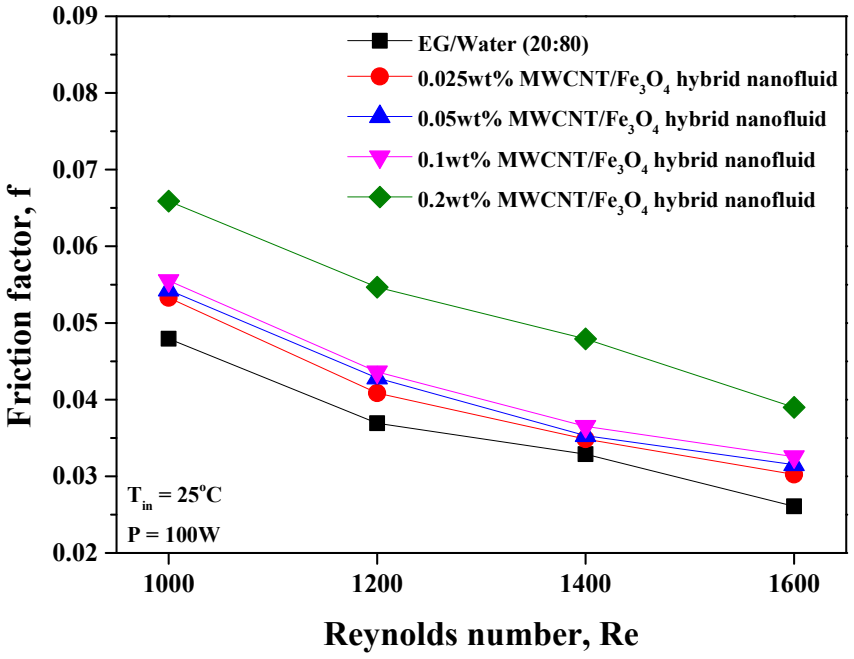

Fig. 3.14 Variation of friction factor with MWCNT/Fe_3O_4 hybrid nanofluids according to the weight concentrations and Reynolds numbers

3.5 Comparison of the convective heat transfer characteristics of MWCNT, Fe_3O_4, and MWCNT/Fe_3O_4 hybrid nanofluids

The comparison of the convective heat transfer coefficients of MWCNT, Fe_3O_4, and MWCNT/Fe_3O_4 hybrid nanofluids according to Reynolds number at the weight concentration of 0.025wt% is shown in Fig. 3.15. The convective heat transfer coefficients of MWCNT, Fe_3O_4 and MWCNT/Fe_3O_4 hybrid nanofluids at a weight concentration of 0.025wt% increased from 1722.2 to 1914.3 W/m^2K as Reynolds numbers increased from 1000 to 1600. Those were increased from 3.9% to 6% in the convective heat transfer coefficient compared to that of the base fluid. It reveals that remarkable improvement in the convective heat transfer coefficient of MWCNT/Fe_3O_4 hybrid nanofluid was shown at a weight concentration of 0.025wt% to compare with MWCNT and Fe_3O_4 nanofluids.

Fig. 3.16 shows the comparison of the convective heat transfer coefficient results of MWCNT, Fe_3O_4, and MWCNT/Fe_3O_4 hybrid nanofluids at the weight concentration of 0.05wt% according to Reynolds number. The convective heat transfer coefficients of MWCNT, Fe_3O_4 and MWCNT/Fe_3O_4 hybrid nanofluids at the weight concentration of 0.05wt% increased from 1730.6 to 1958.5 W/m^2K when the Reynolds number increased from 1000 to 1600. Those were increased from 4.4% to 8.5% in the convective heat transfer coefficient compared to the base fluid. The improvement of convective heat transfer of MWCNT/Fe_3O_4 hybrid nanofluid was 6.9%, 8.1%, 7%, and 8.5%, respectively, when Reynolds numbers was

1000, 1200, 1400 and 1600 at the weight concentration of 0.05wt%.

The comparison of convective heat transfer coefficient of MWCNT, Fe_3O_4, and MWCNT/Fe_3O_4 hybrid nanofluids at the weight concentration of 0.1wt% according to Reynolds number is shown in Fig. 3.17. The convective heat transfer coefficient of MWCNT, Fe_3O_4, and MWCNT/Fe_3O_4 at the weight concentration of 0.1wt% increased from 1792.7 to 2030.5 W/m^2K as Reynolds number increased from 1000 to 1600. Those were increased from 8.2% to 12.4% in the convective heat transfer coefficient compared to the base fluid. The maximum increase in the convective heat transfer coefficient was 2030.5 W/m^2K at the 0.1wt% Fe_3O_4 nanofluid, which was 12.4% higher than the base fluid when Reynolds number was 1600.

Fig. 3.18 shows the convective heat transfer coefficients at the weight concentration of 0.2wt% of MWCNT, Fe_3O_4, and MWCNT/Fe_3O_4 hybrid nanofluids according to Reynolds number. The convective heat transfer coefficients of MWCNT, Fe_3O_4, and MWCNT/Fe_3O_4 hybrid nanofluids at the weight concentration of 0.2wt% increased from 1798.2 to 1988.4 W/m^2K when the Reynolds number increased from 1000 to 1600. Those were increased from 8.5% to 10.1% in the convective heat transfer coefficient compared to the base fluid. It is observed that the improvement of the convective heat transfer coefficient of 0.2wt% MWCNT/Fe_3O_4 hybrid nanofluid was 10.1% higher than that of the base fluid. The improvement of the convective heat transfer coefficient of MWCNT/Fe_3O_4 hybrid nanofluid is restricted by the thermo-physical properties and the random movement of the nanoparticles with the Reynolds number at a high weight concentration of 0.2wt%. Based on these results, the improvement in convective heat transfer is mainly depended on their thermal conductivity, viscosity, thermal

boundary layer, flow condition, shape, and size of the nanoparticle. In all studies of the convective heat transfer, the convective heat transfer coefficient increases with the concentration of the nanoparticles as well as Reynolds number. In this experiment, the convective heat transfer coefficient was dependent on the concentration, and their viscosity. It can be assumed that extra thermal resistance on the inner surface of the test section was caused by the agglomerated Fe_3O_4 nanoparticles, and they coated the inner surface of the test section at high Fe_3O_4 nanofluid concentrations. Besides, the viscosity of the Fe_3O_4 nanofluid increased with the increase of nanofluid concentration. This phenomenon is due to the shear rate in the cross-section of the tube, which reduces the thermal boundary layer thickness.

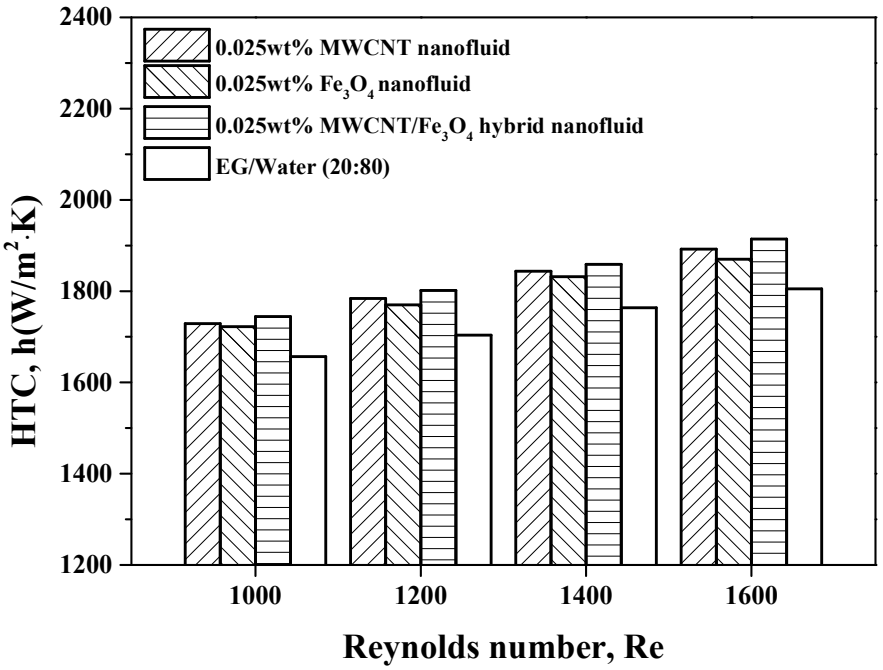

Fig. 3.15 Comparison of the convective heat transfer coefficient of MWCNT, Fe_3O_4, and MWCNT/Fe_3O_4 hybrid nanofluids at a weight concentration of 0.025wt%

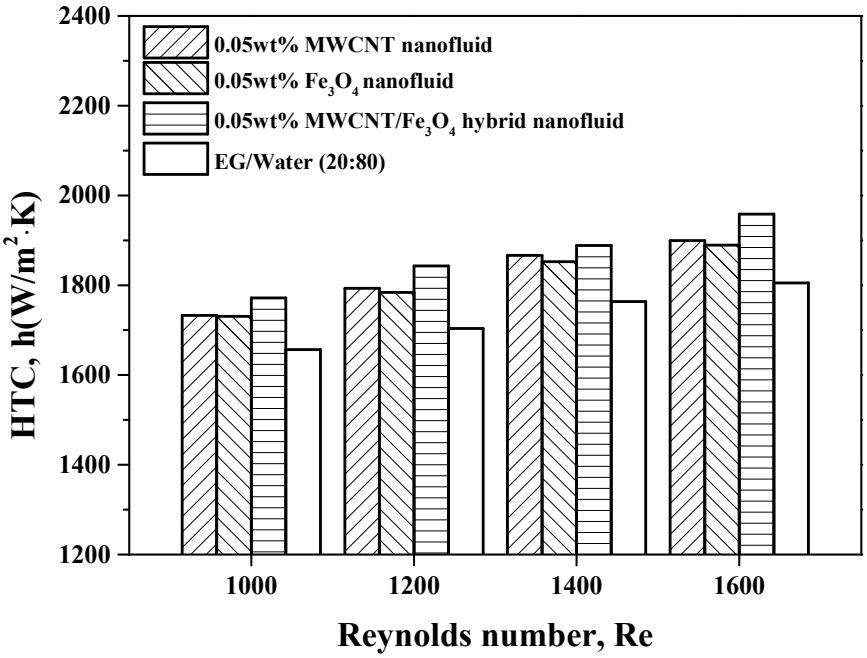

Fig. 3.16 Comparison of the convective heat transfer coefficient of MWCNT, Fe_3O_4, and MWCNT/Fe_3O_4 hybrid nanofluids at a weight concentration of 0.05wt%

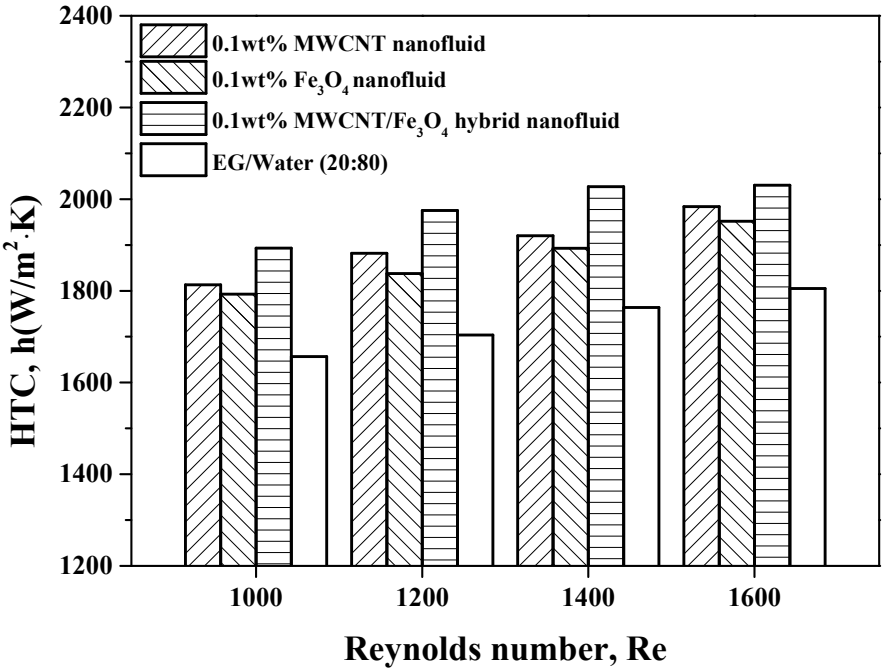

Fig. 3.17 Comparison of the convective heat transfer coefficient of MWCNT, Fe_3O_4, and MWCNT/Fe_3O_4 hybrid nanofluids at a weight concentration of 0.1wt%

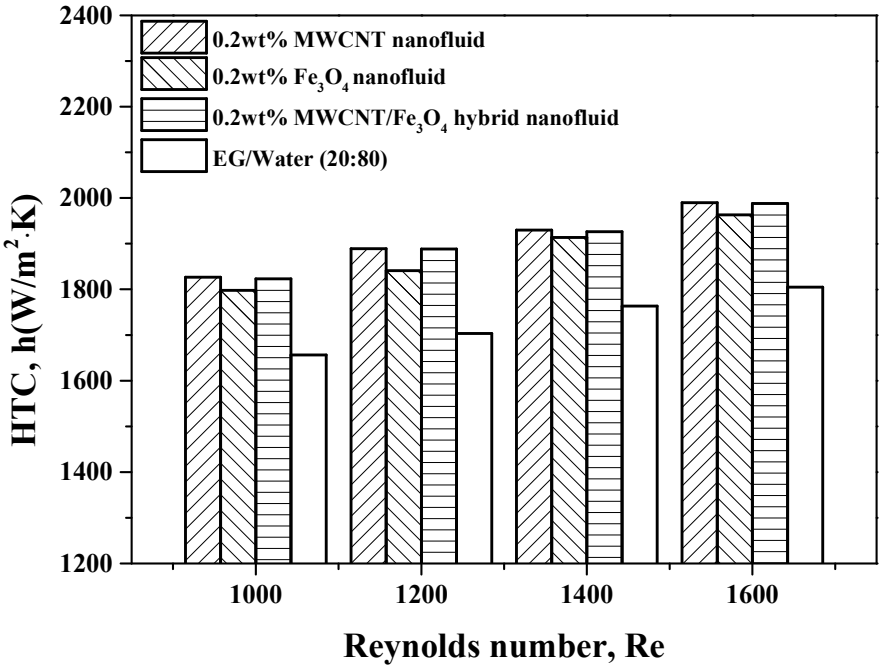

Fig. 3.18 Comparison of the convective heat transfer coefficient of MWCNT, Fe_3O_4, and MWCNT/Fe_3O_4 hybrid nanofluids at a weight concentration of 0.2wt%

The comparison of pressure drop of MWCNT, Fe_3O_4, and MWCNT/Fe_3O_4 hybrid nanofluids according to the Reynolds number at the weight concentration of 0.025wt% is shown in Fig. 3.19. The pressure drop for all nanofluid increased with an increasing of Reynolds number. The pressure drop of MWCNT, Fe_3O_4, and MWCNT/Fe_3O_4 hybrid nanofluid was ranged from 2.96 to 3.1 kPa when Reynolds number increased from 1000 to 1600. Those were increased from 36.7% to 43% in pressure drop compared to the base fluid. It reveals that the maximum increment of pressure drop of MWCNT/Fe_3O_4 hybrid nanofluid was 3.1 kPa which was 43% increased pressure drop at the weight concentration of 0.025wt%.

The pressure drop of MWCNT, Fe_3O_4, and MWCNT/Fe_3O_4 hybrid nanofluids at the weight concentration of 0.05wt% is shown in Fig. 3.20. The pressure drop of MWCNT, Fe_3O_4, and MWCNT/Fe_3O_4 hybrid nanofluid was ranged from 3.09 to 3.16 kPa when Reynolds number increased from 1000 to 1600. Those were increased from 42.6% to 46% in pressure drop compared to the base fluid. The maximum increment of pressure drop of MWCNT/Fe_3O_4 hybrid nanofluid was 3.16 kPa which was 46% increased pressure drop at the weight concentration of 0.05wt%. Besides, the increment of pressure drop of MWCNT, Fe_3O_4, and MWCNT/Fe_3O_4 hybrid nanofluids was 3.09, 3.11, and 3.16 kPa, respectively. Those were 42.6%, 43.3%, and 46% increased one when compared to the base fluid.

Fig. 3.21 shows the pressure drop of MWCNT, Fe_3O_4, and MWCNT/Fe_3O_4 hybrid nanofluids at the weight concentration of 0.1wt% according to Reynolds numbers. The pressure drop of MWCNT, Fe_3O_4, and MWCNT/Fe_3O_4 hybrid nanofluid was ranged from 3.12 to 3.29 kPa when Reynolds number increased from 1000 to 1600. Those were 44.1% to 51.9% increased pressure drop compared to the base fluid. The maximum increment of pressure drop of MWCNT/Fe_3O_4 hybrid nanofluid

was 3.29 kPa which was 51.9% increased pressure drop at the weight concentration of 0.1wt%. In addition, pressure drop enhancement of MWCNT and Fe_3O_4, nanofluids were 44.1% and 47%, respectively, at the weight concentration of 0.1wt% compared to that of the base fluid.

The pressure drop of MWCNT, Fe_3O_4, and MWCNT/Fe_3O_4 hybrid nanofluids according to Reynolds number at the weight concentration of 0.2wt% is presented in Fig. 3.22. The pressure drop of MWCNT, Fe_3O_4, and MWCNT/Fe_3O_4 hybrid nanofluids ranged from 3.24 to 3.52 kPa when Reynolds number increased from 1000 to 1600. Those were 49.6-62.4% increased pressure drop compared to the base fluid. It indicates that the maximum increment of pressure drop was 62.4% in pressure drop of MWCNT/Fe_3O_4 hybrid nanofluid at the weight concentration of 0.2wt%. The increment of pressure drop of MWCNT and Fe_3O_4 nanofluid was 49.6% and 55.2%, respectively, compared to that of the base fluid. From this analysis, the pressure drop of MWCNT, Fe_3O_4, and MWCNT/Fe_3O_4 hybrid nanofluids are higher than that of the base fluid under laminar flow condition, which can increase the pumping power in the system.

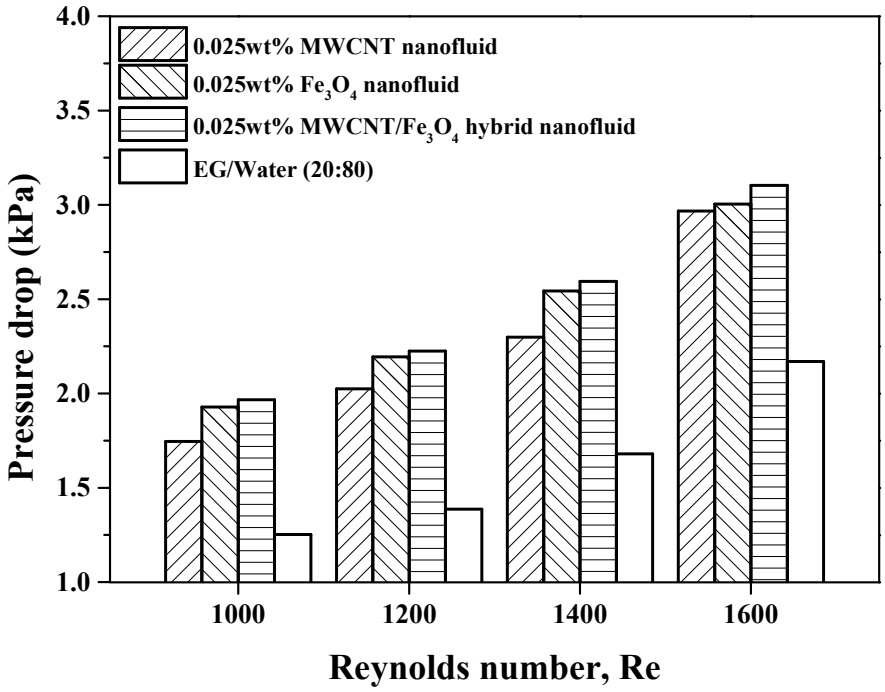

Fig. 3.19 Comparison of pressure drop of MWCNT, Fe_3O_4 and MWCNT/Fe_3O_4 hybrid nanofluids at a weight concentration of 0.025wt%

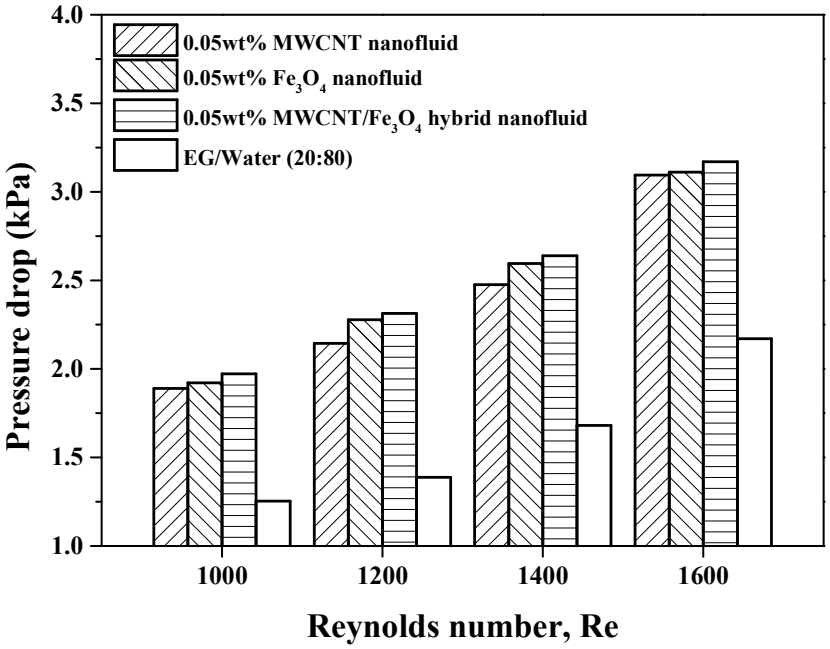

Fig. 3.20 Comparison of pressure drop of MWCNT, Fe_3O_4 and MWCNT/Fe_3O_4 hybrid nanofluids at a weight concentration of 0.05wt%

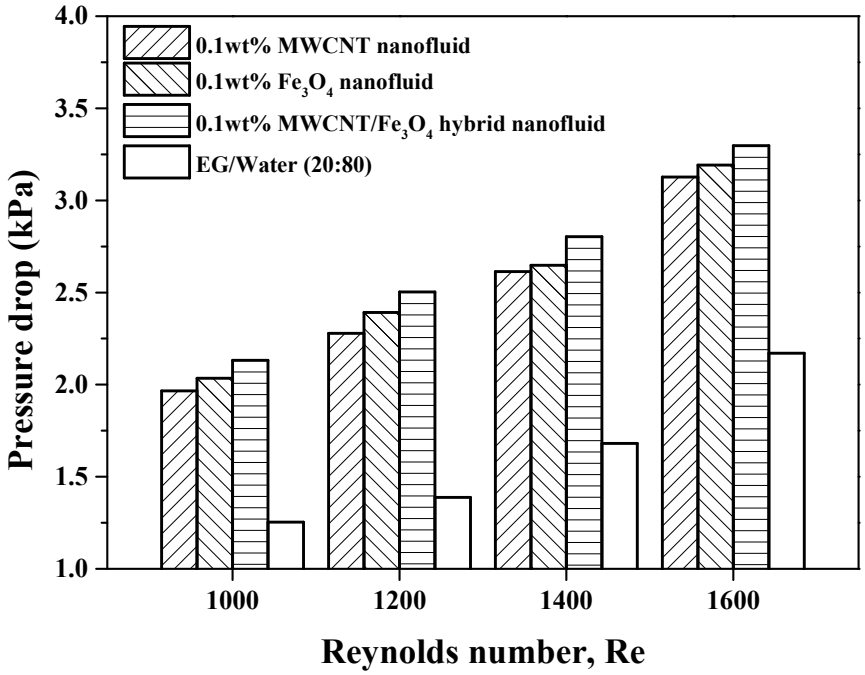

Fig. 3.21 Comparison of pressure drop of MWCNT, Fe_3O_4 and MWCNT/Fe_3O_4 hybrid nanofluids at a weight concentration of 0.1wt%

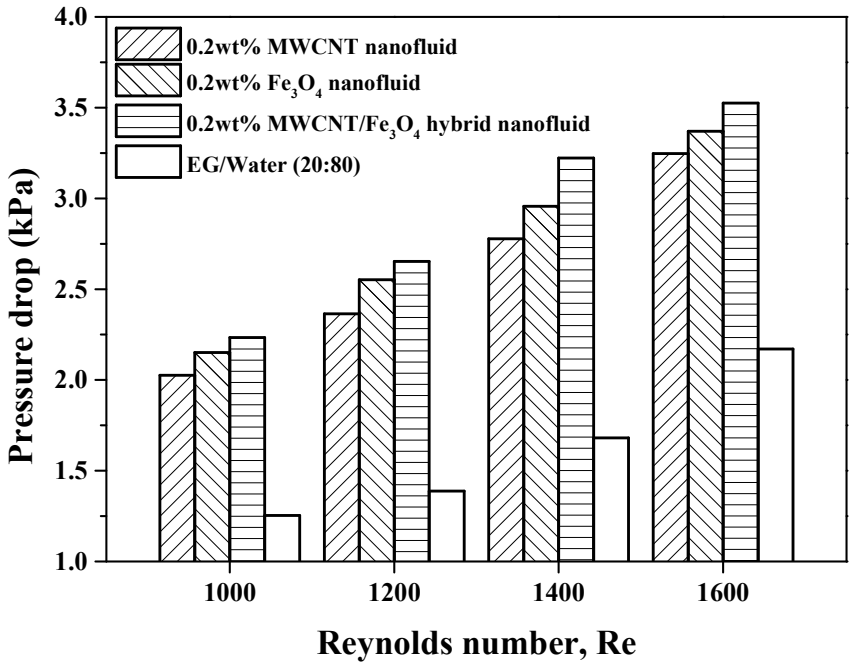

Fig. 3.22 Comparison of pressure drop of MWCNT, Fe_3O_4 and MWCNT/Fe_3O_4 hybrid nanofluids at a weight concentration of 0.2wt%

The comparison of friction factor of MWCNT, Fe_3O_4, and MWCNT/Fe_3O_4 hybrid nanofluids according to Reynolds number at the weight concentration of 0.025wt% is shown in Fig. 3.23. The maximum friction factor of MWCNT/Fe_3O_4 hybrid nanofluid was 0.0331, which was 26.9% increased friction factor at the weight concentration of 0.025wt% as compared with the base fluid. The results observed that the friction factor of MWCNT and Fe_3O_4 nanofluids were 0.0329 and 0.0298 which were 26.2% and 14.5% improved ones, respectively, compared to the base fluid. From this, the Reynolds numbers increased friction factors for all nanofluids.

Fig. 3.24 shows the comparison of friction factor of MWCNT, Fe_3O_4, and MWCNT/Fe_3O_4 hybrid nanofluid. The friction factor of MWCNT, Fe_3O_4, and MWCNT/Fe_3O_4 hybrid nanofluids was ranged from 0.0310 to 0.0339 when Reynolds number increased from 1000 to 1600. Those were 19.1%-30.2% increase in friction factor compared to the base fluid. The friction factor of MWCNT/Fe_3O_4 hybrid nanofluid was 30.2% at the weight concentration of 0.05wt%. Besides, the enhancements of MWCNT and Fe_3O_4 nanofluids were 27.7% and 19.1%, respectively, at the weight concentration of 0.05wt% compared to that of the base fluid.

The comparison of the friction factor of MWCNT, Fe_3O_4, and MWCNT/Fe_3O_4 hybrid nanofluids according to Reynolds number at the weight concentration of 0.1wt% is shown in Fig. 3.25. The friction factor of MWCNT, Fe_3O_4, and MWCNT/Fe_3O_4 hybrid nanofluid was ranged from 0.0320 to 0.0355 when Reynolds number increased from 1000 to 1600. Those were 22.8%-36.3% increase in friction factor compared to that of the base fluid. The enhancements of the friction factor of MWCNT, Fe_3O_4, and MWCNT/Fe_3O_4 hybrid nanofluid was 28.4%, 22.8%, and 36.3%, respectively, compared to that of base fluid.

Comparison of friction factor of MWCNT, Fe_3O_4, and MWCNT/Fe_3O_4 hybrid nanofluids according to Reynolds number at the weight concentration of 0.2wt%, is presented in Fig. 3.26. The friction factor of MWCNT/Fe_3O_4 hybrid nanofluid was 0.0407 which was 56% increased at the weight concentration of 0.2wt% compared to that of the base fluid. The friction factor of MWCNT and Fe_3O_4 nanofluid at a concentration of 0.2wt% was 0.0342 and 0.0355, which were 31.3% and 36% increase in friction factor, respectively, compared to that of base fluid. The fiction factor of MWCNT nanofluid showed little enhancement compared to that of the Fe_3O_4 nanofluid. Besides, the maximum enhancement of friction factor was shown at the 0.2wt% MWCNT/Fe_3O_4 hybrid nanofluid. It can be inferred that the movement of the nanoparticles through the test section due to thermophoresis and Brownian diffusion significantly increases the viscosity of nanofluid, which is flattened velocity. This flattened velocity decreases the temperature difference of the wall and bulk in constant heat flux condition.

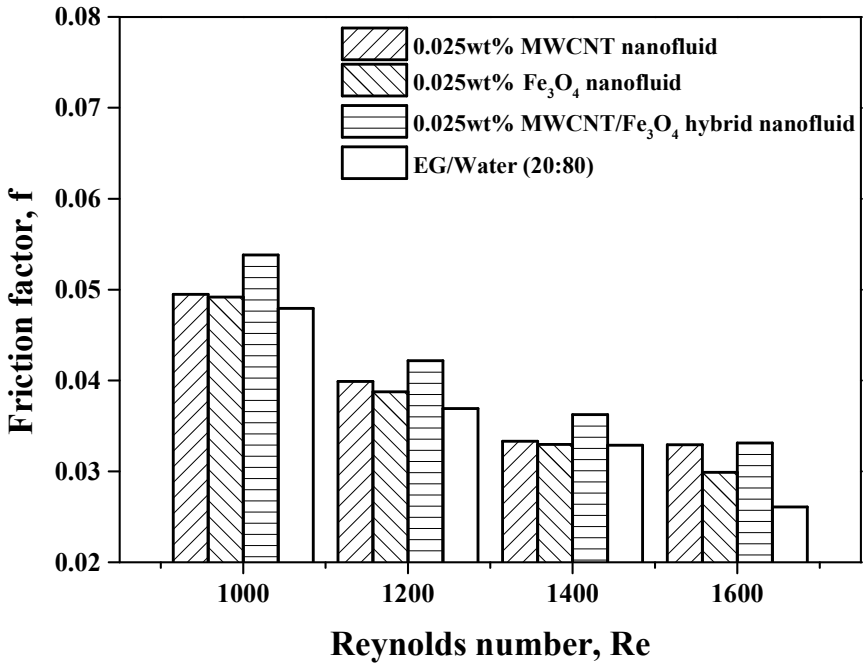

Fig. 3.23 Comparison of friction factor of MWCNT, Fe_3O_4, and MWCNT/Fe_3O_4 hybrid nanofluids at a weight concentration of 0.025wt%

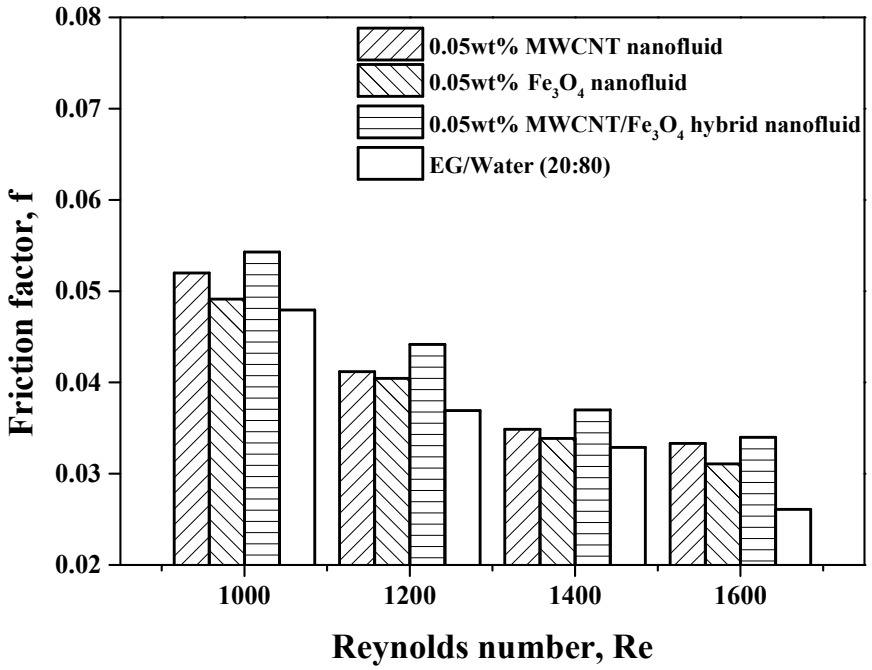

Fig. 3.24 Comparison of friction factor of MWCNT, Fe_3O_4, and MWCNT/Fe_3O_4 hybrid nanofluids at a weight concentration of 0.05wt%

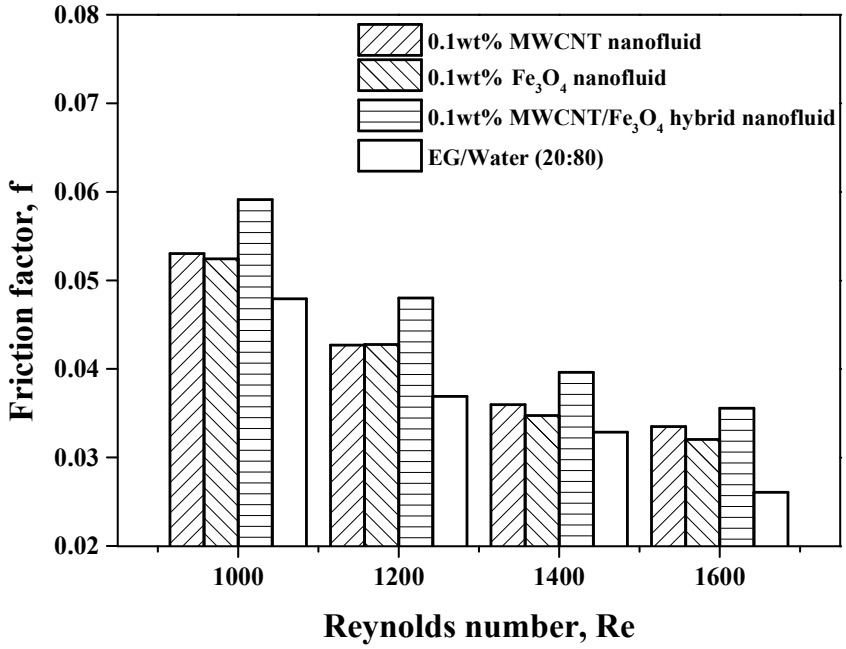

Fig. 3.25 Comparison of friction factor of MWCNT, Fe_3O_4, and MWCNT/Fe_3O_4 hybrid nanofluids at a weight concentration of 0.1wt%

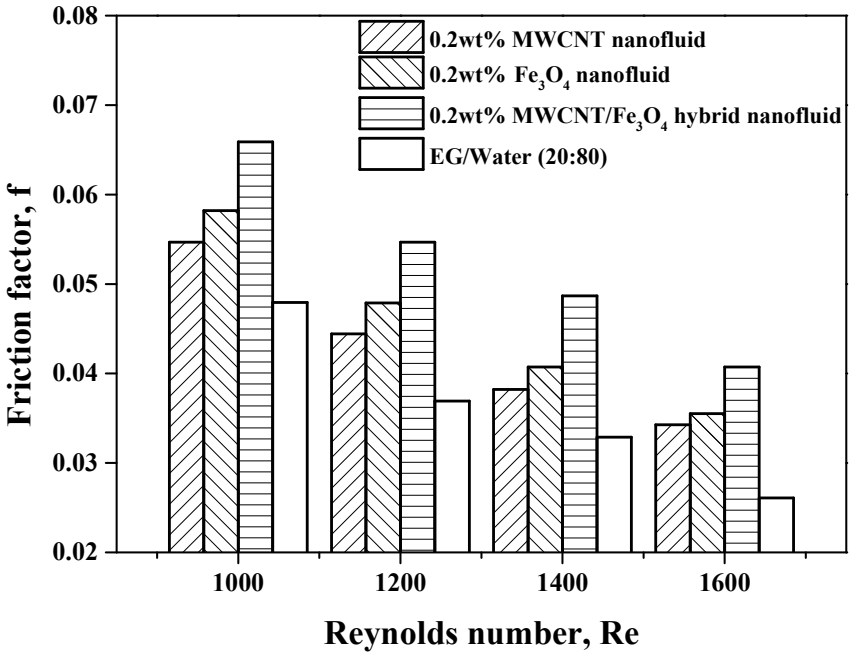

Fig. 3.26 Comparison of friction factor of MWCNT, Fe_3O_4, and MWCNT/Fe_3O_4 hybrid nanofluids at a weight concentration of 0.2wt%

IV. Conclusion

In this study, the convective heat transfer characteristics of MWCNT, Fe_3O_4 and MWCNT/Fe_3O_4 hybrid nanofluids based on EG/Water=20:80 was investigated experimentally. The weight concentrations of nanofluid was ranging from 0.025wt% to 0.2wt% and Reynolds numbers was changed by 1000, 1200, 1400 and 1600, respectively. The Fe_3O_4 nanocomposite synthesized by using the co-precipitation method, which has a magnetic property and has a high potential to improve its thermal properties by adding high thermal conductivity material of MWCNT nanoparticles. Besides, the MWCNT/Fe_3O_4 hybrid nanofluid was fixed at the mixing ratio of 1:1. The following conclusions were made from this investigation.

[1] The convective heat transfer coefficients at the weight concentration of 0.2wt% of MWCNT, Fe_3O_4, and MWCNT/Fe_3O_4 hybrid nanofluids according to Reynolds number was investigated experimentally. The convective heat transfer coefficients of MWCNT, Fe_3O_4, and MWCNT/Fe_3O_4 hybrid nanofluids at the weight concentration of 0.2wt% increased from 1798.2 to 1988.4 W/m^2K when the Reynolds number increased from 1000 to 1600. Those were increased from 8.5% to 10.1% in the convective heat transfer coefficient compared to the basefluid. However, the convective heat transfer coefficient of MWCNT/Fe_3O_4 hybrid nanofluid at a weight concentration of 0.1wt% was 2030.5 W/m^2K, which was 12.4% improvement one compared to the base fluid. It can be assumed that the convective heat transfer coefficient was dependent on the concentration, thermal conductivity, and viscosity. The particle migration effect was occurred when the viscosity of nanofluid increased with

the increase of nanofluid concentration. This particle migration can be due to the shear rate in the cross section of tube, which increase the thermal boundary layer thickness. In addition, the increasing concentration of nanofluid leads to reduce the dispersion stability of MWCNT/Fe_3O_4 hybrid nanofluid at weight concentration of 0.2wt%, therefore the convective heat transfer performance decreases.

[2] In general, the MWCNT/Fe_3O_4 hybrid nanofluid is more effective in increasing the convective heat transfer coefficient compared to single nanofluids of MWCNT and Fe_3O_4. In comparison, the MWCNT/Fe_3O_4 hybrid nanofluid was found to have the highest convective heat transfer coefficient and pressure drop. The highest flow velocity was also obtained in the MWCNT/Fe_3O_4 hybrid nanofluid. As a result, the velocity of MWCNT/Fe_3O_4 hybrid nanofluid can be increased to increase the intensity of synergistic effect which is the heat convection intensity factor of convective heat transfer enhancement.

[3] All nanofluids had a higher convective heat transfer coefficient compared to the base fluid. The convective heat transfer coefficient increased with an increase in the Reynolds number and nanoparticle concentration. The improvement of convective heat transfer were occurred in the entry length region. This improvement in the entrance region was caused by the low thermal boundary layer thickness because the effect of viscous shear rate gradually spread further away from the wall to the centerline. In this study, the friction factor of MWCNT/Fe_3O_4 hybrid nanofluid was 0.0407 which was 56% increased friction factor at the weight concentration of 0.2wt% compared

to that of the base fluid. The friction factor of MWCNT and Fe_3O_4 nanofluid at a concentration of 0.2wt% was 0.0342 and 0.0355, which were 31.3% and 36% increased friction factor, respectively, compared to that of base fluid. Friction factor was decreased with the increase of Reynolds number. The increasing nanofluid concentration with an increase in nanofluid viscosity, which decreased fluid movement. It can be inferred that the movement of the nanoparticles through the test section increased because thermophoresis and Brownian diffusion significantly increased of nanofluid, which was flattened velocity. This flattened velocity decreased the temperature difference of the wall and bulk in constant heat flux condition.

REFERENCE

[1] S. Saallah, I. W. Lenggoro, "Nanoparticles carrying biological molecules: recent advances and applications" KONA Powder and Particle Journal, vol. 35, 89-111, 2018.

[2] S.U.S. Choi, J.A. Eastman, "Enhancing thermal conductivity of fluids with nanoparticles" ASME Fed, vol. 1, 99-105, 1995.

[3] J. T. Cieslinski, P. Kozak, "Experimental investigation of forced convection of water/EG-Al_2O_3 nanofluids inside horizontal tube" E3S Web of Conferences, vol. 70, 1-5, 2018.

[4] A. V. Minakov, A. S. Lobasov, D. V. Guzei, M. I. Pryazhnikov, V. Y. Rudyak, "The experimental and theoretical study of laminar forced convection of nanofluids in the round channel" Applied Thermal Engineering, vol. 88, 140-148, 2015.

[5] M. Gupta, R. Kumar, N. Arora, S. Kumar, N. Dilbagi, "Forced convective heat transfer of MWCNT/Water nanofluid under constant heat flux: An experimental investigation" Arabian Journal for Science and Engineering, vol. 41, 599-609, 2015.

[6] A. Chiney, V. Ganvir, B. Rai, Pradip, "Stable nanofluids for convective heat transfer applications" Journal of Heat Transfer, vol. 136, 021704-1-7, 2014.

[7] K. B. Anoop, T. Sundararajan, S. K. Das, "Effect of particle size on the convective heat transfer in nanofluid in the developing region" International Journal of Heat and Mass Transfer, vol. 52, 2189-2195, 2009.

[8] W. Yu, D. M. France, S. Smith, D. Singh, E. V. Timofeeva, J. L. Routbort, "Heat transfer to a silicon carbide/water nanofluid" International Journal of Heat and Mass Transfer" vol. 52, 2272-2281, 2009.

[9] B. Mehrjou, S. Z. Heris, K. Mohamadifard, "Experimental study of CuO/water nanofluid turbulent convective heat transfer in square cross-section duct" Experimental Heat Transfer: A Journal of Thermal Energy Generation, Transport, Storage, and Conversion, vol. 28-3, 282-297, 2015.

[10] S. Z. Heris, S. G. Etemad, M. S. Esfahany, "Experimental investigation of oxide nanofluids under laminar flow convective heat transfer" International Communications of Heat and Mass Transfer, vol. 33, 529-535, 2006.

[11] C. K. Mangrulkar, V. M. Kriplani, A. S. Dhoble, "Experimental investigation of convective heat transfer enhancement using alumina/water and copper oxide/water nanofluids" Thermal Science, vol. 20, 1681-1692, 2016.

[12] V. Kumaresan, S. M. A. Kander, S. Karthikeyan, R. Velraj, "Convective heat transfer characteristics of CNT nanofluids in a tubular heat exchanger of various lengths for energy efficient cooling/heating system" International

Journal of Heat and Mass Transfer, vol. 60, 413-421. 2013.

[13] D. Wen, Y. Ding, "Formulation of nanofluids for natural convective heat transfer applications" International Journal of Heat and Fluid Flow, vol. 26, 855-864, 2005.

[14] S. Ferrouillat, A. Bontemps, J. P. Ribeiro, J. A. Gruss, O. Soriano, "Hydraulic and heat transfer study of SiO_2/water nanofluids in horizontal tubes with imposed wall temperature boundary conditions." International Journal of Heat and Fluid Flow, vol. 32, 424-439, 2011.

[15] H. C. Shin, S. Han, S. M. Kim, "Numerical study on the forced convection heat transfer of nanofluids in micro-channels" Journal of Nanoscience and Nanotechnology, vol. 17, 8394-8403, 2017.

[16] H. F. Oztop, E. A. Nada, Y. Varol, K. A. Salem, "Computational analysis of non-isothermal temperature distribution on natural convection in nanofluid filled enclosures" Superlattices and Microstructures, vol. 49, 453-467, 2011.

[17] M. Kalteh, K. Javaherdeh, T. Azarbarzin, "Numerical solution of nanofluid mixed convection heat transfer in a lid-driven square cavity with a triangular heat source" Powder Technology, vol. 253, 780-788, 2014.

[18] R. Azizian, E. Doroodchi, T. McKrell, J. Buongiorno, L. W. Hu, B. Moghtaderi, "Effect of magnetic field on laminar convective heat transfer of magnetite

nanofluids" International Journal of Heat and Mass Transfer, vol. 68, 94-109, 2014.

[19] L. S. Sundar, M. K. Singh, A. C. M. Souca, "Thermal conductivity of ethylene glycol and water mixture based Fe_3O_4 nanofluid" International Communications in Heat and Mass Transfer, vol. 49, 17-24, 2013.

[20] H. Zhu, C. Zhang, S. Liu, Y. Tang, Y. Yin, "Effects of nanoparticle clustering and alignment on thermal conductivities of Fe_3O_4 aqueous nanofluids" Applied Physics Letters, vol. 89, 023123, 2006.

[21] A. Ghofrani, M. H. Dibaei, A. H. Sima, M. B. Shafii, "Experimental investigation on laminar forced convection heat transfer of ferrofluids under an alternating magnetic field" Experimental Thermal and Fluid Science, vol. 49. 193-200, 2013.

[22] L. Sha, Y. Ju, H. Zhang, "The influence of the magnetic field on the convective heat transfer characteristics of Fe_3O_4/water nanofluids, Applied Thermal Engineering, vol. 126, 108-116, 2017

[23] M. Asfer, B. Mehta, A. Kumar, S. Khandekar, P. K. Panigrahi, "Effect of magnetic field on laminar convective heat transfer characteristics of ferrofluid flowing through a circular stainless-steel tube" International Journal of Heat and Fluid Flow, vol. 59, 74-86, 2016.

[24] H. Sadrhosseini, A. Sehat, M. B. Shafii, "Effect of magnetic field on internal forced convection of ferrofluid flow in porous media" Experimental Heat Transfer: A Journal of Thermal Energy Generation, Transport, Storage, and Conversion, vol. 29, 1-16, 2015.

[25] D. Guzei, A. Minakov, M. Pryazhnikov, K. Meshkov, "Investigating the forced convection of magnetic nanofluids" MATEC Web of Conferences 115, 1-4, 2017.

[26] M. Ashjaee, M. Goharkhah, L. A. Khadem, R. Ahmadi, "Effect of magnetic field on the forced convection heat transfer and pressure drop of a magnetic nanofluid in a miniature heat sink" Heat Mass Transfer, Springer-Verlag Berlin Heidelberg, 2014.

[27] M. Goharkhah, M. Ashjaee, M. Shahabadi, "Experimental investigation on convective heat transfer and hydrodynamic characteristics of magnetite nanofluid under the influence of an alternating magnetic field" International Journal of Thermal Sciences, vol. 99, 113-124, 2016.

[28] M. Yarahmadi, H. M. Goudarzi, M. B. Shafii, "Experimental investigation into laminar forced convective heat transfer of ferrofluids under constant and oscillating magnetic field with different magnetic field arrangements and oscillation modes" Experimental Thermal and Fluid Science, vol. 68, 601-611, 2015.

[29] N. Hatamia, A. K. Banari, A. Malekzadeh, A. R. Pouranfard, "The effect of magnetic field on nanofluids heat transfer through a uniformly heated horizontal tube" Physics Letters A, vol. 1, 1-6, 2016.

[30] A. Shahsavar, M. Saghafian, M. R. Salimpour, M. B. Shafii, "Experimental investigation on laminar forced convective heat transfer of ferrofluid loaded with carbon nanotubes under constant and alternating magnetic fields" Experimental Thermal and Fluid Science, vol. 76, 1-11, 2016.

[31] L. Shi, Y. He, Y. Hu, X. Wang, "Controllable natural convection in a rectangular enclosure filled with Fe_3O_4@CNT nanofluids" International Journal of Heat and Mass Transfer, vol. 140, 399-409, 2019.

[32] B. Takabi, H. Shokouhmand, "Effects of Al_2O_3-Cu/water hybrid nanofluid on heat transfer and flow characteristics in turbulent regime" International Journal of Modern Physics, vol.26, 1550047-1-25, 2015.

[33] H. H. Balla, Sh. Abdullah, W. Mohdfaizal, R. Zulkifli, K. Sopian, "Numerical study of the enhancement of heat transfer for hybrid CuO-Cu nanofluids flowing in a circular pipe" Journal of Oleo Science, vol. 62, 533-539, 2013.

[34] M. N. Labib, M. J. Nine, H. Afrianto, H. Chung, H. Jeong, "Numerical investigation on effect of base fluids and hybrid nanofluid in forced convective heat transfer" International Journal of Thermal Sciences, vol. 71, 163-171, 2013.

[35] A. A. Minea, "Challenges in hybrid nanofluids behavior in turbulent flow: Recent research and numerical comparison" Renewable and Sustainable Energy Reviews, vol. 71, 426-434, 2017.

[36] C. Uysal, E. Gedik, A. J. Chamkha, "A numerical analysis of laminar forced convection and entropy generation of a diamond-Fe_3O_4/water hybrid nanofluid in a rectangular mini channel" Journal of Applied Fluid Mechanics, vol.12, 391-402, 2019.

[37] L. M. Al-Balushia, M. J. Uddinb, M. M. Rahm, "Natural convective heat transfer in a square enclosure utilizing magnetic nanoparticles" Propulsion and Power Research, vol. 8, 194-209, 2019.

[38] J. Alsarraf, R. Rahmani, A. Shahsavar, M. Afrand, S. Wongwises, M. D. Tran "Effect of magnetic field on laminar forced convective heat transfer of MWCNT-Fe_3O_4/water hybrid nanofluid in a heated tube" Journal of Thermal Analysis and Calorimetry, Springer, 2019.

[39] B. C. Pak, Y. I. Cho, "Hydrodynamic and heat transfer study of dispersed fluids with submicron metallic oxide particles" Experimental Heat Transfer, vol. 11 151-170, 1998.

[40] T. G. Beckwith, R. D. Marangoni, J. H. Lienhard, "Mechanical measurements", 5th edition, Wesley Publishing Company, 1993.

[41] R. K. Shah, A. L. London, “Laminar flow forced convection in ducts” A Source Book for Compact Heat Exchanger Analytical Data, 1978.

[42] H. Yarmand, S. Gharehkhani, G. Ahmadi, S. F. S. Shirazi, S. Baradaran, E. Montazer, M. N. M. Zubir, M. S. Alehashem, S. N. Kazi, M. Dahari, “Graphene nanoplatelets-silver hybrid nanofluids for enhanced heat transfer, vol. 100, 419-428, 2015.

Acknowledgement

First of all, I would like to express my sincere gratitude to my advisor, Honghyun Cho for the continuous support and advice. His guidance helped me in all the time of research and writing of this work. It would not have been possible to do this study without the help of my professor's advice, support, and suggestions.

Especially, thank you for Dr. Chonggyun Ham and Areum Lee, their help, and invaluable support during my thesis work. I unfailingly remember the all-time.

Above all, I would like to thank members of the R.E.L for their personal support and helps at all times. I am very grateful to a number of people, who have been helped me in getting this thesis to completion. I wish to express my gratitude to Dr. Yunchan Shin, Dr. Tsogtbilegt Boldoo, Daewon Jang, Minjung Lee, Woobin Kang, and other members for spending their valuable time on helping and supporting me to my work and life in Korea.